

アルツハイマー病の対症療法開発を目的とした

$\beta$ -シート構造ターミネーターの合成

(研究課題番号 12650861)

平成 12 年度～平成 13 年度科学研究費補助金(基盤研究(C)(2))

研究成果報告書

平成 14 年 3 月

研究代表者 山 田 哲 弘

(千葉大学 教育学部 助教授)

## は し が き

Alzheimer 病患者の脳組織中には老人斑と呼ばれる独特の斑が観察される。この斑はアミロイドが蓄積したもので本疾病の要因と考えられている。アミロイドは $\beta$ -シートで構造化されたオリゴペプチドの超分子であるから、分子間水素結合をターミネートできれば破壊できるはずである。

アミロイドの破壊を研究するならば、市販もされている現実の $\beta$ -アミロイドペプチドは不可欠のように考えられる。だが、危険性が危惧される現実の $\beta$ -アミロイドペプチドは高価でもあり、複雑なシーケンス（一次構造）のため二次構造解析も容易ではない。つまり、単純なモデルを利用すれば、分子レベルでアミロイドの崩壊を安価かつ安全に研究できる可能性が高い。

幸いなことに、著者が研究を続けてきたペプチド型両親媒性分子はアミロイドモデルとして利用できそうであった。このことから、本研究ではペプチド型両親媒性分子が作る超分子をアミロイドモデルとして位置づけ、Alzheimer 病の対症療法薬を開発する上での新しい提案を行う目的で、ペプチド間水素結合を破壊する作用、あるいは水素結合形成を抑制する機能を持った水素結合ターミネーター分子を探索・合成した。

本研究で得られた成果は大別して以下の二つであり、本成果報告書はこれらについての詳細をまとめたものである。

1. アミロイドモデルに位置づけたペプチド型両親媒性分子の会合体について詳細な検討を加えた結果、この会合体の形成メカニズムや構造上の特徴に新たな知見が得られたこと。
2. プロトンドナーが欠落したアミノ酸のペプチドを共存させることにより、 $\beta$ -シート構造で連鎖したアミロイド状の会合体を断片化できること。

## 研究組織

研究代表者：山田哲弘（千葉大学教育学部助教授）

（研究協力者：花本綱；千葉大学大学院教育学研究科 平成12年度修了生）

（研究協力者：小松司；千葉大学大学院教育学研究科 在学中）

（研究協力者：田上勇一；千葉大学教育学部学生 平成13年度卒業予定）

## 交付決定額（配分額）

（金額単位：千円）

	直接経費	間接経費	合計
平成12年度	3000	0	3000
平成13年度	700	0	700
総計	3700	0	3700

## 研究発表

### (1) 学会誌等

#### 1. Norihiro Yamada, Katsuhiko Ariga

“Formation of  $\beta$ -Sheet Assemblage with a View to Developing an Amyloid Model”

*Synlett*, **2000**, (No.5), 575-586

#### 2. 山田哲弘, 有賀克彦

“ペプチド脂質の特異的構造形成”

*油化学*, **49**, No.5, 435-446 (2000)

#### 3. Norihiro Yamada, Kazuhiro Matsubara, Kikou Narumi, Yo-ichi Sato, Emiko Koyama, Katsuhiko Ariga

“Lyotropic Aggregate of Tripeptide Derivatives within Organic Solvents: Study on Dynamic Property of Molecular Assembling”

*Colloids Surf., A* **169**, (No.1-3), 271-285 (2000)

#### 4. Katsuhiko Ariga, Jun-ichi Kikuchi, Masanobu Naito, Emiko Koyama, Norihiro Yamada

“Modulated Supramolecular Assemblies Composed of Tripeptide Derivatives: Formation of Micrometer-Scale Rods, Nanometer-Size Needles, and Regular Patterns with Molecular-Level Flatness from the Same Compound”

*Langmuir*, **16**, (Issue 11), 4929-4939 (2000)

山田哲弘

“有機溶媒中における会合体形成のメカニズムおよびオルガノゲルとの関連”

高分子加工, 第 49 巻, 第 8 号, 338-343 (2000)

5. Katsuhiko Ariga, Jun-ichi Kikuchi, Masanobu Naito, Norihiro Yamada  
FT-IR, TEM, and AFM Studies on Supramolecular Architecture Formed by  
Tripeptide-Containing Amphiphiles

*Polym. Adv. Technol.* **11**, (Issue 8-12), 856-864 (2000)

6. 山田哲弘

“分子集合体によるオルガノゲル形成と構造評価”

ネットワークポリマー, 第 21 巻, 第 4 号, 199-206 (2000)

7. Norihiro Yamada, Tamae Imai, and Emiko Koyama

“Lyotropic Aggregate of Tripeptide Derivatives within Organic Solvents:  
Relationship between Interpeptide Hydrogen Bonding and Packing Arrangements  
of Components”

*Langmuir*, **17**, (Issue 4), 961-963 (2001)

(2) 口頭発表

1. 山田哲弘・佐藤洋一

“ペプチド脂質を用いたメタノール中での二分子膜形成”

日本化学会第 78 春季年会 (日本大学理工学部船橋キャンパス)

2000 年 3 月 29 日

講演予稿集 I, p.17 (2 A1 30)

2. 山田哲弘・花本綱・小松司・田上勇一

“ペプチド型両親媒性分子の水素結合連鎖制御”

第 50 回高分子討論会 (早稲田大学大久保キャンパス)

2001 年 9 月 12 日

高分子学会予稿集, Vol.50, (No.8), pp.1554-1555 (ID04)

3. 山田哲弘・小松司・吉永浩嗣

“分子の三次元座標制御による超分子フィルムの形成”

第 50 回高分子討論会 (早稲田大学大久保キャンパス)

2001 年 9 月 12 日

高分子学会予稿集, Vol.50, (No.11), pp.2416-2417 (IK16)

4. 山田哲弘・花本綱・田上勇一

“プロトンドナーを欠く低分子量ペプチドを用いた $\beta$ -シート集積体の崩壊”

第16回生体機能関連化学シンポジウム（千葉大学西千葉キャンパス）

2001年9月20日

講演要旨集, pp.38-39 (1S2-05)

5. 高橋京子・山田哲弘

“ペプチド型両親媒性分子の気水界面単分子膜形成”

日本化学会第80秋季年会（千葉大学西千葉キャンパス）

2001年3月22日

講演予稿集, p.322 (3 P6A-09)

6. 山田哲弘

“水素結合とロイシンジッパーの強相関低分子フィルム”

文部科学省科学研究費補助金 特定領域研究 (A) 「強相関マテリアルの動的制御」, 平成13年度第二回公開シンポジウム（名古屋大学シンポジオンホール）

2002年1月28日

要旨集, pp.96-97

7. 小松司・吉永浩嗣・高橋京子・山田哲弘

“ロイシンジッパーと水素結合形成能を有する低分子フィルム素材”

第51回高分子学会年次大会（パシフィコ横浜）

2002年5月30日（発表予定）

高分子学会予稿集, Vol.51, (IIPa139)

## 研究成果

### 1 研究目的

何らかの要因で変成した蛋白分子やその断片が分解されずに臓器中で蓄積すると、蓄積した臓器の機能不全を誘発する。蓄積物はアミロイド (Amyloid)<sup>1)</sup> と呼ばれ、疾病はアミロイドーシス (Amyloidosis) と総称されるが、蓄積した部位を冠して心アミロイドーシス、腎アミロイドーシスなどと呼ばれる。近年社会問題になっている Alzheimer 病もアミロイドーシスの一種である。Alzheimer 病の場合、アミロイドは脳神経細胞の周りに蓄積し、結果である機能不全は痴呆となって現れる。

アミロイドは異常に安定である。正常な蛋白と異なり、タンパク質加水分解酵素群の作用を受けないだけでなく、熱的にも安定であるとされる。しばしばアミロイド線維とも呼ばれるように、その形態の多くは繊維状であり、繊維長軸方向に連鎖した水素結合、詳細に言えば蛋白分子の二次構造の一種である  $\beta$ -シートで構造固定されている。形成過程に細菌やウイルスの関与が論じられることもあるが、アミロイドそのものはペプチドの集積物であるという点で化学的な物質である。このことは、アミロイドーシスが化学的な手法によって駆逐しうる疾病であることを暗示しているように思える。構造特性から考えて、アミロイドは水素結合を崩壊させることができれば除去できる。ペプチド間の水素結合はプロトンドナーの N-H 基とプロトンアクセプターの C=O 基との間に形成される。そこで、プロトンドナーを欠くペプチドを混合すれば、このペプチドが水素結合連鎖の末端に結合したとき、以後の連鎖は停止すると考えた。本研究では、プロトンドナーを欠くペプチド分子を水素結合ターミネーターと称し、実際の効果を検討することが第一の目的である。

このアイディアを実践するにあたっては問題点が一つあった。アミロイドの入手である。アミロイドを形成する実際のペプチド (これを  $\beta$ -Amyloid peptide と言う) は、シーケンスが解明されているものあり、市販もされている。しかし、Alzheimer 病と同様、異常な蛋白が疾病要因となっているクロイツフェルト・ヤコブ病 (CJD) などいわゆるプリオン病を考えた場合、現実の  $\beta$ -アミロイドペプチドを用いるのは、高価であるということのほか感染に対する不安がぬぐえない。周知のように、一度できた異常プリオンやアミロイドは核になって自発的に集積するからである。そこで、まず安価・安全かつ大量に使用できるアミロイドモデルが必要となった。

著者らが研究しているトリペプチド型両親媒性分子 (図 1) は、水中・有機溶媒中で会合体を形

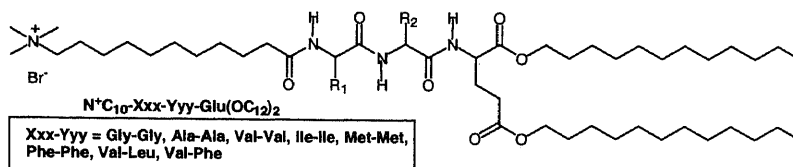


図 1 トリペプチド型両親媒性分子

成するが、幸いなことにこの会合体は形態がアミロイドに酷似している。しかも、 $\beta$ -シートで構造化されている点は、アミロイドとの最大の共通点となっている。これらのことから本研究では、まずペプチド型両親媒性分子の会合体について構造をより詳細に検討し、新しいアミロイドモデルとして利用可能であることを提案した。この提案の詳細については別添総説 (*Synlett*, 2000, (No.5), 575-586) を参照いただきたい。次いで、提案したアミロイドモデルに先の水素結合ターミネーターを添加して水素結合の連鎖停止作用を検討した。

## 2 研究の背景と方法

### 2-1 トリペプチド型両親媒性分子についての概略

はじめにトリペプチド型両親媒性分子の概略を述べる必要があるだろう。この分子は図1に示すようにグルタミン酸ジドデシルエステルと 11-トリメチルアンモニウムウンデカノイル基を共通構造として有する。二つの共通構造はジペプチドで連結されており、グルタミン酸を含めるとトリペプチド基を有することになる。以下、この分子をトリペプチド型両親媒性分子と称し、トリペプチドのシーケンスをもって略号とする。詳細は拙著論文<sup>2)</sup>に譲るとして、トリペプチド型両親媒性分子は、水中のみならず、四塩化炭素 ( $\text{CCl}_4$ )、ベンゼン、トルエン、シクロヘキサンなどの無極性有機溶媒中でも会合体を形成する。溶液の外観は水溶液が散乱溶液、有機溶媒溶液はゲルである。溶媒を問わず会合体中のペプチド部には平行 $\beta$ -シート構造が形成されており、フーリエ変換赤外 (FT-IR) スペクトルから簡便に証明できる。

例として、図2に会合体を含む  $\text{CCl}_4$  および水中の FT-IR スペクトルと会合体が形成されないクロロホルム ( $\text{CHCl}_3$ ) 溶液の FT-IR スペクトルを示した<sup>2c)</sup>。3280  $\text{cm}^{-1}$

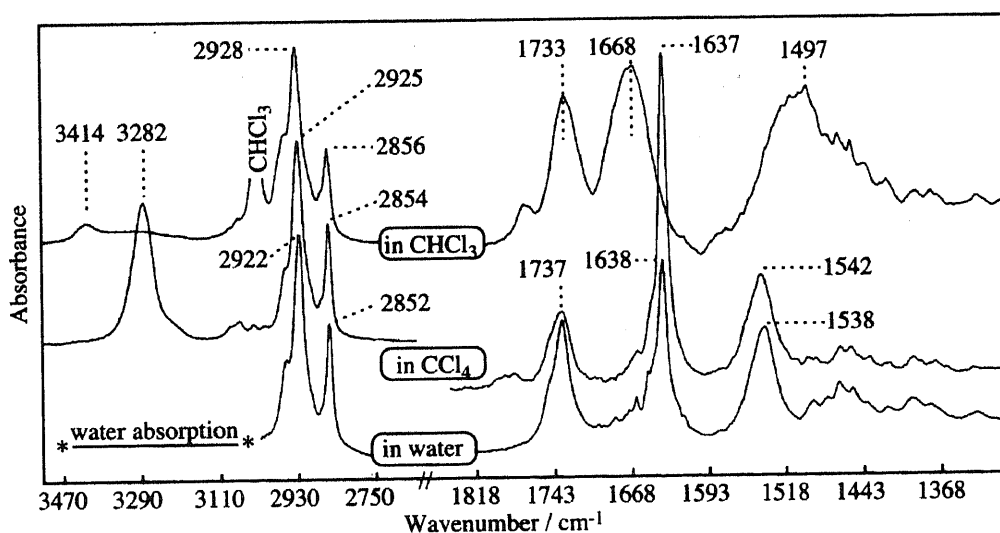
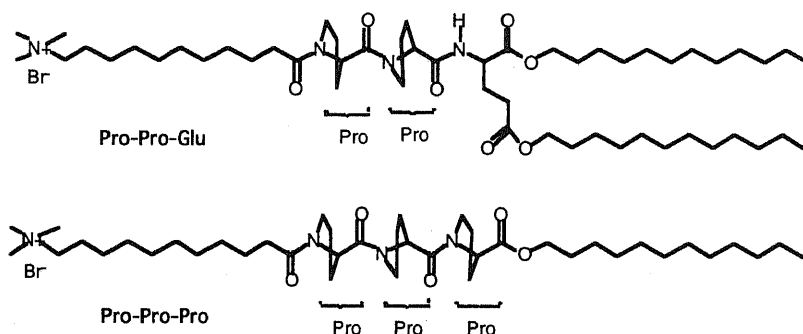


図2 Phe-Phe-Glu 型両親媒性分子の FT-IR スペクトル [2c]

シート構造の特徴的吸収である。ペプチド部に平行β-シート構造が形成されている限り、分子は水中で二分子膜構造<sup>3)</sup>、有機溶媒中で逆二分子膜構造を形成していることになる。透過型電子顕微鏡観察の結果によればトリペプチド型両親媒性分子の会合形態は繊維であるから<sup>2d)</sup>、水素結合はミセル繊維あるいは逆ミセル繊維の長軸方向に形成されている。以上の概略の詳細に関しては別添総説（油化学, 49, No.5, 435-446 (2000)）を参照いただきたい。

## 2-2 水素結合連鎖制御の手法および評価

本研究では、二個のプロトンドナーが欠落した **Pro-Pro-Glu** 型両親媒性分子と三個のプロトンドナーが欠落した **Pro-Pro-Pro** 型両親媒性分子を合成し（以下これらの分子をターミネーター分子と



総称する), これをβ-シートで構成された先のアミロイドモデルに添加することで水素結合連鎖の停止を試みた(図3)。水素結合の連鎖を断ち切ることで、会合体崩壊を計画したが、このような手法が試みられたことはない。

アミロイドモデルは有機溶媒をゲル化させるが、水素結合連鎖が抑制されれば会合体が成長しないため、ゲルのもととなる繊維状会合体が形

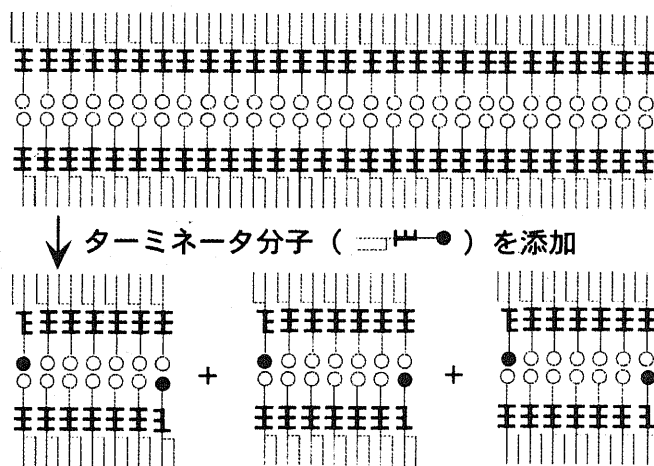


図3 ターミネーター分子の添加による水素結合連鎖の切断

成されず、ゲルは粘性の低い溶液に変化すると考えられた。この現象は直裁的に肉眼で観察できるはずである。定量的評価に関しては、当初、水素結合が分断された場合、FT-IR スペクトルにおいて未会合状態のアミドが増加するため、会合種から非会合種へのスペクトルシフトが起こると予想した。しかし、ターミネーター分子はプロトンドナーを欠くもののプロトンアクセプターを有するから、単独では会合しないとしても、アミロイドモデル分子（例えば **Val-Val-Glu** 型両親媒性分子）のプ



ロトンドナーとは水素結合できる。このため、ターミネーター分子の溶液中と Val-Val-Glu 型両親媒性分子の溶液中に存在する非会合および会合性アミド基の総数は、たとえ連鎖停止機能が働いたとしても混合前後で変化しない。むしろ、連鎖停止が起こった場合、結果として生ずる会合体中の分子パッキングが変化し、いくつかの官能基の吸収体がシフトする変化となって現れることがわかった。これらの点については後述する。

### 3 結果

#### 3-1 リオトロピック液晶としてのトリペプチド型両親媒性分子

実際のアミロイドについて、紹介されている電子顕微鏡写真を見ると、繊維状である以外、構造規則性は見られない。この点から考えれば、アミロイドは結晶ではなく、リオトロピック液晶としての分子集合体であるように思われる。アミロイドが結晶であるか液晶であるかは、アミロイド研究においていずれは大きな意味合いをもって来るだろうが、現時点ではこの点に言及した研究報告は少ない。本研究でも、トリペプチド型両親媒性分子が作る会合体をアミロイドモデルとして利用する場合、それが液晶であるか結晶であるかをまず明確にする必要があったが、FT-IR スペクトルを詳細に解析した結果、有機溶媒中の繊維状会合体が結晶ではなくリオトロピック液晶であることを明らかにした。詳細は添付論文 (*Langmuir*, 17, (Issue 4), 961-963 (2001)) を参照いただきたい。

#### 3-2 トリペプチド型両親媒性分子の会合に対する水素結合の役割

水素結合連鎖の崩壊を検討するに当たり、本研究では分子会合に対する水素結合の役割についても検討を加えた。水素結合基を含む分子が自己会合するケースでは、概して水素結合を会合の駆動力と考えがちである。複数の水素結合基有する有機化合物が自己会合しやすい傾向にあることは事実であるが、多くの場合、多重水素結合は結晶化に有利である。水素結合は、それとは別の相互作用によって集合した分子間に形成されて、集合構造を固定する役割を担っている。トリペプチド型両親媒性分子の有機溶媒中における会合では、よく知られた逆相ミセルの形成と同様の相互作用で分子集合した後、隣接する分子間に水素結合が形成されるものと考えられる。これらに関する研究成果については別添論文 (*Colloids Surf., A* 169, (No.1-3), 271-285 (2000) ; 高分子加工 第 49 巻, 第 8 号, 338-343 (2000) ; ネットワークポリマー, 第 21 巻, 第 4 号, 199-206 (2000)) を参照いただきたい。

### 3-3 ターミネーター分子の合成

ターミネーター分子は、これまで合成を行ってきたトリペプチド型両親媒性分子と異なって第三アミド結合を有する。第三アミド結合は、アミノ酸残基を N-末端に逐次縮合する合成法を採用した場合、保護基である Boc 基を HBr/酢酸等の強酸で除去する際に開裂してしまうようである。このため、図4に示したように N-末端保護基の除去が必要ない合成法、あるいは図5に示したように Z 基を接触還元によって切断する合成法を採用した。この方法で得た中間生成物・最終生成物は FT-IR スペクトルと  $^1\text{H-NMR}$  スペクトルから構造確認したが、図4に示した最終生成物は、満足できる元素分析結果を与えたものの  $^1\text{H-NMR}$  はわずかながらラセミ化を示唆するスペクトルを与えた。また、図5の最終生成物は元素分析の結果が理論値と実測

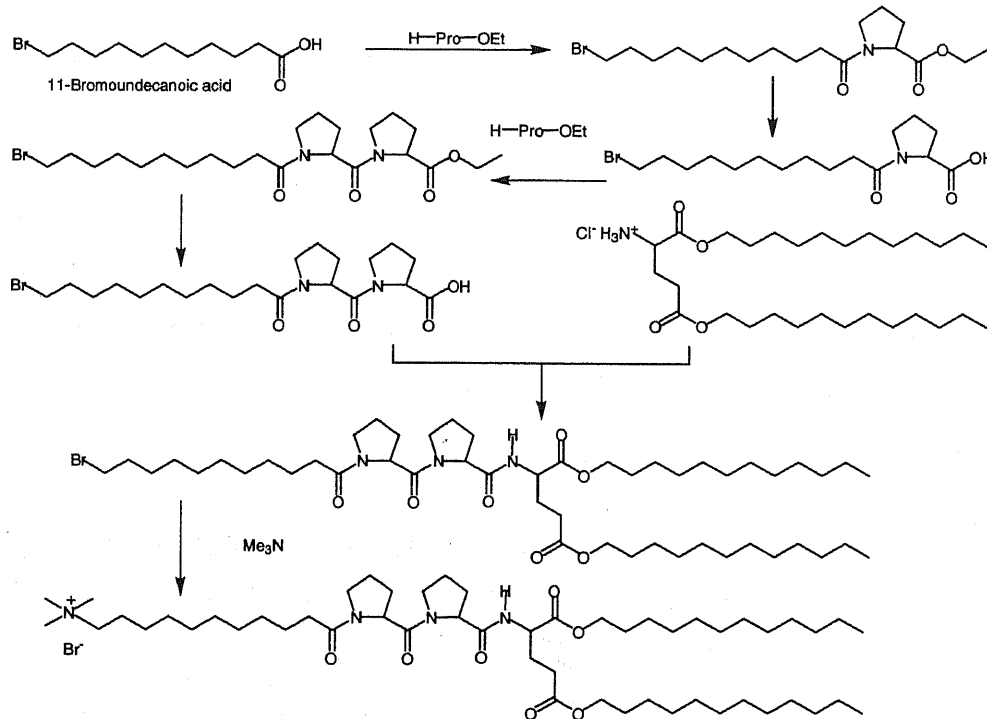


図4 Pro-Pro-Glu 型両親媒性分子の合成スキーム

値の間で 0.3%以上の差を生じた。

ターミネーター分子の場合、最終生成物・中間体ともに油状物であることが多く、精製が難しい。これは今後の課題であるが、ゲルパーミエーションクロマトグラフィーなどの手法で精製を考える必要がある。このように、純度の点では問題を残すものの、 $\beta$ -シート構造の断片化を検討したところ当初期待したとおりの結果が得られた。従って、次節に述べたようにターミネーター分子の効果そのものは実証することができた。

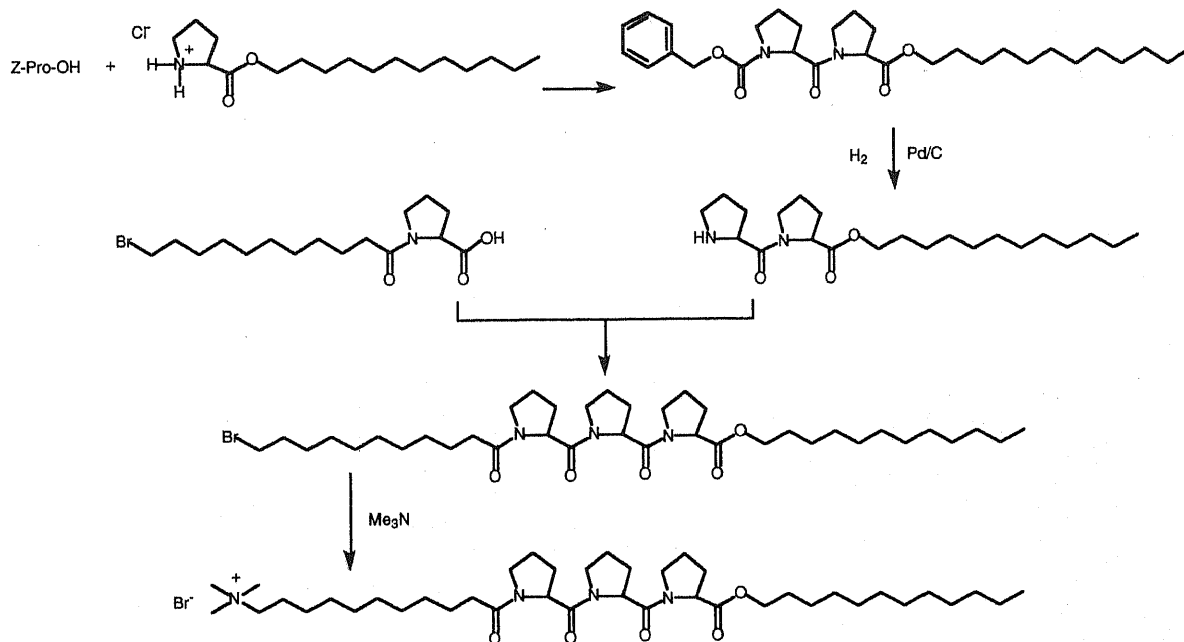


図5 Pro-Pro-Pro 型両親媒性分子の合成スキーム

### 3-4 水素結合のターミネート

Pro-Pro-Glu 型両親媒性分子を Phe-Phe-Glu 型両親媒性分子が作る会合体に加えたところ、ゲルの崩壊が肉眼で観察できた。図6は、Phe-Phe-Glu を  $\text{CCl}_4$  に分散させ

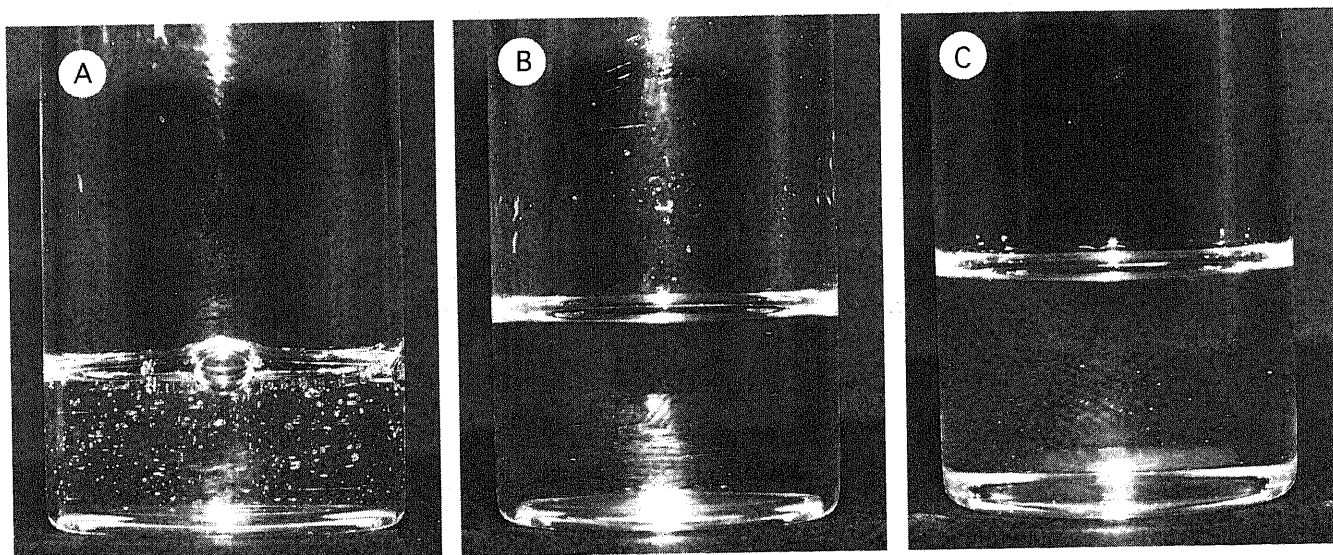


図6 オルガノゲル(A)のターミネーター(B)添加による崩壊(C): (A) Phe-Phe-Glu の  $2\text{ mM-CCl}_4$  溶液、(B) Pro-Pro-Glu の  $2\text{ mM-CCl}_4$  溶液、(C) (A) と (B) を等量混合した直後

た際形成されるゲル (図6A) と Pro-Pro-Glu 型両親媒性分子の  $\text{CCl}_4$  溶液 (図6B) とを混合し、ゲルが崩壊の様子を記録したものである (図6C)。溶液を激しく振り混ぜて泡立てると、溶液がゲルの場合は取り込まれた気泡がそのままゲル中に停

留した状態になる (図 6 A)。ゲルではない溶液の場合, 取り込まれた気泡は液中を素早く上昇し, 残留することはない (図 6 B)。図 6 C は気泡を取り込んだゲルが **Pro-Pro-Glu** 型両親媒性分子の添加によって透明溶液に変化したものである。

図 7 は **Phe-Phe-Phe** 型両親媒性分子の繊維状会合体 (図 7 A) が **Pro-Pro-Pro** 型両親媒性分子の添加によって断片化したところ (図 7 B) を微分干渉顕微鏡で観察したものである。これらの結果は, プロトンドナーを欠落させた構造類似の分子が, 水素結合連鎖を停止させる作用を持つことの証拠である。

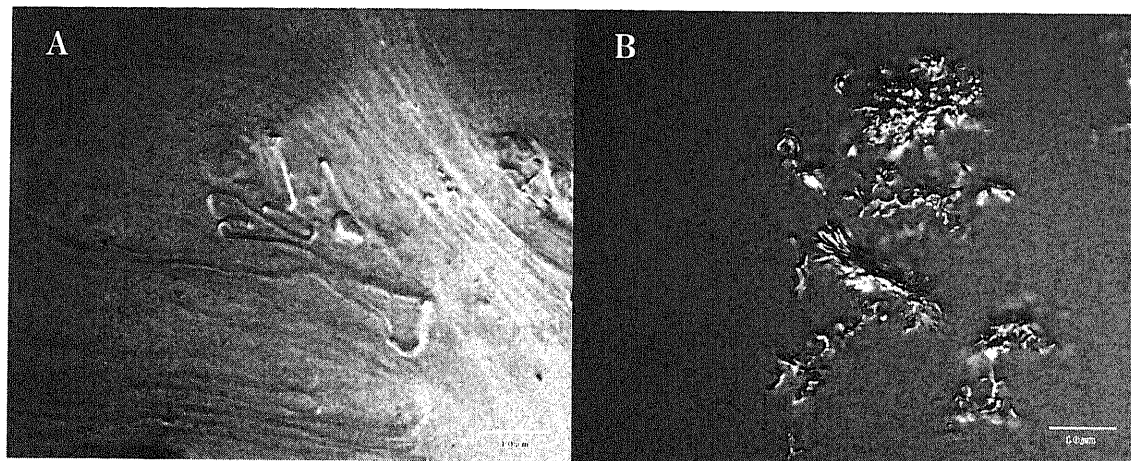


図 7 ターミネータ分子による繊維状構造の断片化  
(A) **Phe-Phe-Phe** の繊維状会合体 (4 mM- $\text{CCl}_4$  溶液)  
(B) **Phe-Phe-Phe** + **Pro-Pro-Pro** (**Phe-Phe-Phe** は 2 mM, **Pro-Pro-Pro** は 4 mM である)。

### 3-5 水素結合連鎖停止の定量的評価

しかしながら, 肉眼観察のみでは, 水素結合連鎖の停止効果を定量的に評価できない。そこで, FT-IR スペクトルの変化から水素結合崩壊の定量的評価を試みたが, 崩壊の検出を明確な形でとらえることはできなかった。研究の背景と方法の項でも述べたように, 当初は未会合アミド吸収体の強度がゲル崩壊に連動して増加すると考えた。しかし, 系中の会合アミドと未会合アミドの割合は, ターミネータ分子とゲルの混合前後で変化しない。例えば, **Pro-Pro-Glu** 型両親媒性分子のプロトンアクセプターは **Phe-Phe-Glu** 型両親媒性分子プロトンドナーと結合して水素結合連鎖を停止する。このとき, **Pro-Pro-Glu** と **Phe-Phe-Glu** の間に水素結合が形成されるので, **Phe-Phe-Glu** 型両親媒性分子の水素結合が崩壊しても **Pro-Pro-Glu** 型両親媒性分子との水素結合が増加して, 水素結合数は見かけ上変化しない。しかし, FT-IR スペクトルの測定によって興味深いデータも得られた。**Pro-Pro-Glu** 型両親媒性分子の場合, 水素結合は Pro-Glu 結合のアミド基部分でしか形成されないため, 平行  $\beta$ -シート構造が形成されないことはもちろんであるが, 有機溶媒中での自己会合も期

待できない分子であった。事実、**Pro-Pro-Glu** 型両親媒性分子は、 $\text{CCl}_4$  に分散しても溶液はゲル化しない。この場合、FT-IR スペクトルにおいてアミド I のすべては未会合のはずであるが、**Pro-Pro-Glu** のアミドは  $1680\text{ cm}^{-1}$  と  $1642\text{ cm}^{-1}$  の二本に分裂した(図 8)。後者は明らかに会合性アミドの吸収である。このことから、**Pro-Pro-Glu** 型両親媒性分子は溶液をゲル化させることはないものの、何らかの会合体を形成し

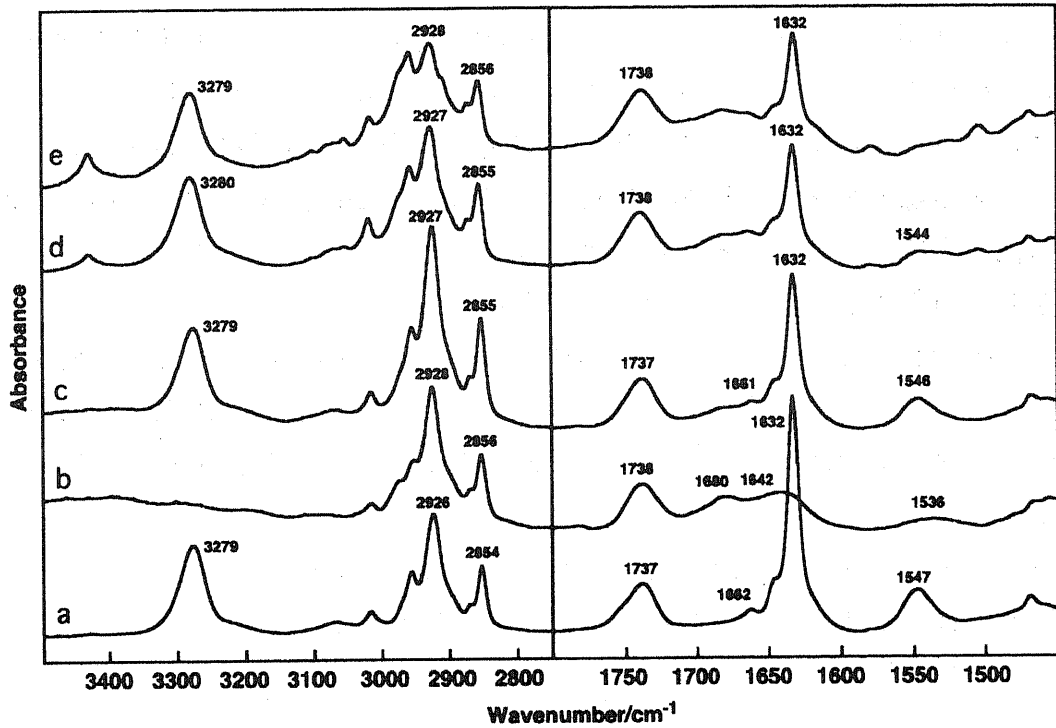


図 8 **Pro-Pro-Glu** 型両親媒性分子 (ターミネーター) および **Val-Val-Glu** 型両親媒性分子の  $\text{CCl}_4$  中における FT-IR スペクトルと混合に伴う変化 : a **Val-Val-Glu** 型両親媒性分子の  $2\text{ mM-CCl}_4$  溶液、b **Pro-Pro-Glu** 型両親媒性分子の  $2\text{ mM-CCl}_4$  溶液、c a と b を加算したスペクトル、d **Pro-Pro-Glu** 型両親媒性分子と **Val-Val-Glu** 型両親媒性分子を等量混合して 1 時間後、e **Pro-Pro-Glu** 型両親媒性分子と **Val-Val-Glu** 型両親媒性分子を等量混合して 12 時間後

ていることがわかる。ただし、ピークは非常にブロードであり、形成されている水素結合は構造規則性に乏しいものである。会合性から非会合性アミドへのシフトと言う観点からは、水素結合崩壊の検出をできなかったが、図 8 に示したように、ターミネーター分子の添加によって  $\text{CH}_2$  伸縮振動が著しくブロード化した。 $\nu_{\text{as}}\text{CH}_2$  と  $\nu_{\text{s}}\text{CH}_2$  の高波数シフトとブロード化はアルキル鎖の流動性増大を意味する。したがって、図 8 の結果は、水素結合連鎖の崩壊に伴って構造規則性をもった会合体 (ここではゲルを形成している繊維状会合体) も崩壊し、アルキル鎖の流動性が増加したことを示唆している。このデータは、図 6・図 7 の結果とあわせ、計画したターミネーター分子に水素結合の連鎖停止作用があることを示唆するものである。

#### 4 まとめ

本研究で得られた成果と新たに生じた問題点を以下にまとめた。

まず、成果から述べる。本研究は、アミロイドーシスの対症療法薬の開発を目指し、アミロイドの構造安定化因子である水素結合の崩壊を検討したものであるが、安全・安価・大量に利用することができる新規アミロイドモデルの提案とターミネーター分子による水素結合連鎖抑制効果の確認を主要な課題とした。形態・構造の類似性から新規アミロイドモデルとして提案したトリペプチド型両親媒性分子は、各種の溶媒中でリオトロピック液晶を形成することが新たにわかり、アミロイドとの共通性はさらに深まった。この他、本研究の主題とは若干離れるものの、トリペプチド型両親媒性分子の有機溶媒中における会合挙動は、現在大きな興味を持たれている低分子量分子によるオルガノゲル形成<sup>4)</sup>に対して、ゲル形成のメカニズムや物性解明に貢献するところが大きいこともわかった。ターミネーター分子による水素結合連鎖抑制についても、ゲルの崩壊という直裁的観察結果からその効果を明らかにできた。これまで、水素結合に連鎖停止という観点からの研究は行われたことがなく、本研究での成果は、様々な水素結合系において会合数制御に応用できそうである。

ターミネーター分子の精製は問題点の一つである。また、FT-IR スペクトル法による解析が満足できるものではないため、連鎖抑制の効果を定量的に解析する手段の開発も必要である。

#### 6 引用文献

- 1) アミロイド、プリオンについては、次の文献が詳しい。  
“Amyloid, Prions, and Other Protein Aggregates”; Wetzel, R., Ed.; Methods in Enzymology Vol. 309; Academic Press Inc.: San Diego, 1999.
- 2) a) Yamada, N.; Koyama, E.; Kaneko, M.; Seki, H.; Ohtsu, H.; Furuse, T. *Chem. Lett.* **1995**, 387; b) Yamada, N.; Koyama, E.; Maruyama, K. *Kobunshi ronbunshu*, **1995**, 52, 629; c) Yamada, N.; Koyama, E.; Imai, T.; Matsubara, K.; Ishida, S. *J. Chem. Soc., Chem. Commun.* **1996**, 2297; d) Yamada, N.; Ariga, K.; Naito, M.; Matsubara, K.; Koyama, E. *J. Am. Chem. Soc.* **1998**, 120, 12192; e) Yamada, N.; Matsubara, K.; Koyama, E.; Fujioka, M., *Chem. Lett.* **1997**, 1033.
- 3) Kunitake, T. *Angew Chem. Int. Ed. Engl.* **1992**, 31, 709.
- 4) Terech, P.; Weiss, R. G. *Chem. Rev.* **1997**, 97, 3133.

# Formation of $\beta$ -Sheet Assemblage with a View to Developing an Amyloid Model

Norihiro Yamada,<sup>a,\*</sup> Katsuhiko Ariga<sup>b</sup>

<sup>a</sup> Faculty of Education, Chiba University, 1-33 Yayoi-cho, Inage-ku, Chiba 263-8522, Japan

<sup>b</sup> Graduate School of Materials Science, Nara Institute of Science and Technology (NAIST), 8916-5 Takayama, Ikoma, Nara 630-0101, Japan

Received 23 June 1999

**Abstract:** Amphiphilic molecules that contain a tripeptide moiety form an aggregate not only in water but also in organic solvents. The aggregate possesses fibrous morphology and involves a rich amount of parallel  $\beta$ -sheet structure of peptides, which is similar to a  $\beta$ -amyloid peptide called an amyloid fibril. The dynamic properties of the aggregate of the tripeptide-containing amphiphiles were also similar to those of the amyloid. These similarities suggest that the tripeptide-containing amphiphiles are suitable for an amyloid model.

1	Introduction
2	Amyloid and Its Models
2.1	Molecular Design
2.2	Preparation and Diagnostics
3	Static Properties of $\beta$ -Sheet Assemblage
3.1	Macroscopic Observations
3.2	Microscopic Observations
3.3	$\beta$ -Sheet Structure
3.3.1	Parallel-Chain $\beta$ -Sheet Structure
3.3.2	Antiparallel-Chain $\beta$ -Sheet Structure
4	Dynamic Properties of $\beta$ -Sheet Assemblage
4.1	Critical Concentration
4.2	Thermal Stability
4.3	Catalyzing Effect
4.4	Hydrophobic Tripeptide Derivatives
5	Conclusion

**Key words:** amyloid,  $\beta$ -sheet structure, organogel, hydrogen bonding, peptide-containing amphiphile

## 1 Introduction

Inappropriate mutation of normal cellular proteins generates fragmentary peptides or abnormal disease-causing isoforms (prion peptides).<sup>1</sup> The small peptides sometimes self-assemble into an amyloid fibril, which accumulates in various internal organs and causes functional diseases called amyloidosis. The amyloid has been known to be related to prion diseases (CJD, GSS, FFI etc), Alzheimer's disease, Huntington's disease, Parkinson's disease<sup>1</sup> and many other conventional amyloidoses such as renal amyloidosis. Because these are fatal diseases, it is very important to find the pathogenesis and the therapeutics of these diseases.<sup>2</sup>

In order to study amyloidosis, a real amyloid is ideally required. The majority of studies, hence, employed various types of synthetic oligopeptides,<sup>3-6</sup> for example, leucine-rich repeat oligopeptides<sup>4</sup> and ionic self-complementary oligopeptides,<sup>5</sup> as a model of the mutant proteins. Aggeli

suspects that all of the gel-forming oligopeptides could also be applied to the amyloid model.<sup>6</sup> However, it is not easy to prepare the oligopeptide forming a desired secondary structure, because all of the oligopeptides adopt an inherent secondary structure depending upon the kinds of component amino acids and their number. Furthermore, it is difficult to analyze the secondary structure of the oligopeptides that possess a complicated primary structure and various amino acid residues.

Therefore, a simpler peptide which produces an amyloid-like structure is required to attempt breaking the restriction described above. From this viewpoint, we have proposed a new amyloid model using tripeptide-containing amphiphiles. Because the tripeptide-containing amphiphiles contain only a few kinds of amino acid residues, structural analyses, particularly the mode of the interpeptide hydrogen bonding, should become easy. We have described in this paper the details of why the aggregate of the tripeptide-containing amphiphiles is suitable for the amyloid model.

## 2 Amyloid and Its Models

The amyloid is an assemblage of peptide fragments, whose morphological figure is a fibril. As reported for the Alzheimer's  $\beta$ -amyloid peptide, all of the component peptides are perpendicular to the fiber axis.<sup>7</sup> The molecular arrangement is immobilized by the interpeptide hydrogen bonding, and hence, the amyloid contains a rich amount of  $\beta$ -sheet structure. This  $\beta$ -sheet domain often catalyzes the further conversion of segments from the  $\alpha$ -helix to the  $\beta$ -sheet form.<sup>1,8</sup> In this manner, the amyloid fibril multiplies. Once the amyloid fibril is integrated, it is very difficult to disintegrate because the amyloid possesses chemical and/or thermal stability. Although the latent period of the amyloidosis is extremely long, the amyloid steadily multiplies during the period. The resultant accumulation of the amyloid fibrils never spontaneously disappears. These facts show that the monomeric peptide fragments and their aggregate (amyloid fibril) should not coexist at equilibrium, and hence, the amyloid fibril should be a spontaneous assemblage, that is to say, a self-assembly.

According to the general features of the amyloid, its model must be a fibrous self-assemblage based on the  $\beta$ -sheet structure, which has thermal stability and a catalyzing effect to convert the other secondary structures of peptides.

## 2.1 Molecular Design

It has been known that an amphiphilic molecule (surfactant) can form a bilayer structure in water.<sup>9</sup> Figure 1 includes two types of the local structures of a bilayer membrane, namely a normal bilayer structure (A) and an interdigitated monolayer structure (B).<sup>10,11</sup> Regardless of these types, the long axes of the component molecules orientate perpendicular to the two-dimensional film-plane. If a peptide group is introduced into the amphiphile, interpeptide H-bonding should be easily formed between the nearest neighboring molecules. We then designed and prepared the following molecules (Chart 1). These molecules possess a hydrophilic ammonium group, a tripeptide group, and one or two hydrophobic alkyl chains. Fortunately, the tripeptide-containing amphiphiles formed an aggregate not only in water but also in some nonpolar organic solvents.<sup>12-14</sup> The local structure of the aggregate in organic media should be a reversed bilayer structure as illustrated in Figure 1(C). The adjacent neighboring tripeptides should be arranged parallel to each other in the normal bilayer (A') and in the reversed bilayer (C) membrane. In contrast, the adjacent neighboring tripeptides should be arranged either parallel or antiparallel to each other in the interdigitated monolayer membrane (Figure 1(B')). Therefore, we can obtain a parallel and an antiparallel  $\beta$ -sheet structure by controlling the solvent-polarity and/or molecular orientation.

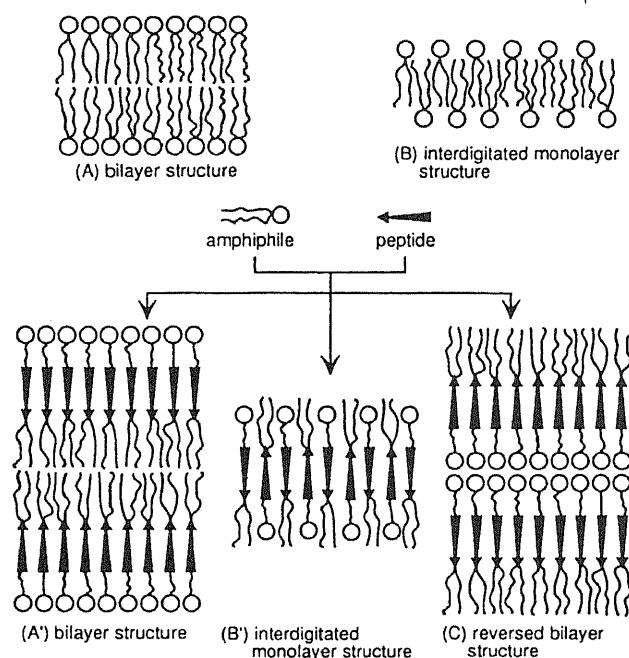
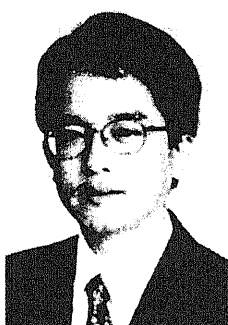


**Figure 1** Different possibilities of arranging tripeptide-containing amphiphiles.

## Biographical Sketches



**Norihiro Yamada** was born in Kyoto in 1957, and was educated at the Science University of Tokyo. From 1980-1982 he studied with Professor Shigeru Oae at Tsukuba University and re-

ceived his MSc. in chemistry in 1982. Subsequently, he worked with Professor Toyoki Kunitake at Kyushu University and obtained his Ph.D. in 1985. At that time, he was appointed to re-

search associate at Kyushu University. He served as lecturer at Chiba University since 1986, and as Associate Professor from 1989.



**Katsuhiko Ariga** was born in Matsudo, a city in the Tokyo Metropolitan area, Japan, in 1962. He received his B. Eng. degree in 1984, M. Eng. degree in 1986, and a Ph.D. degree in 1990 (supervisor, Prof. Yoshio Okahata) from Tokyo Institute of Technology. He worked as research associate at TITEC (Prof. Okahata), as a

postdoctoral fellow at University of Texas at Austin (Prof. Eric V. Anslyn), as group leader in the Supermolecules Project, Japan Science and Technology Corporation (Prof. Toyoki Kunitake), as researcher in the Core Research for the Evolution Science and Technology Program, JST (Prof. Yasuhiro Aoyama),

and then was served as Associate Professor at Nara Institute of Science and Technology (NAIST). His research interests include two-dimensional space technology, specific functions at interfaces, supramolecular structure of lipids, and origin of life.



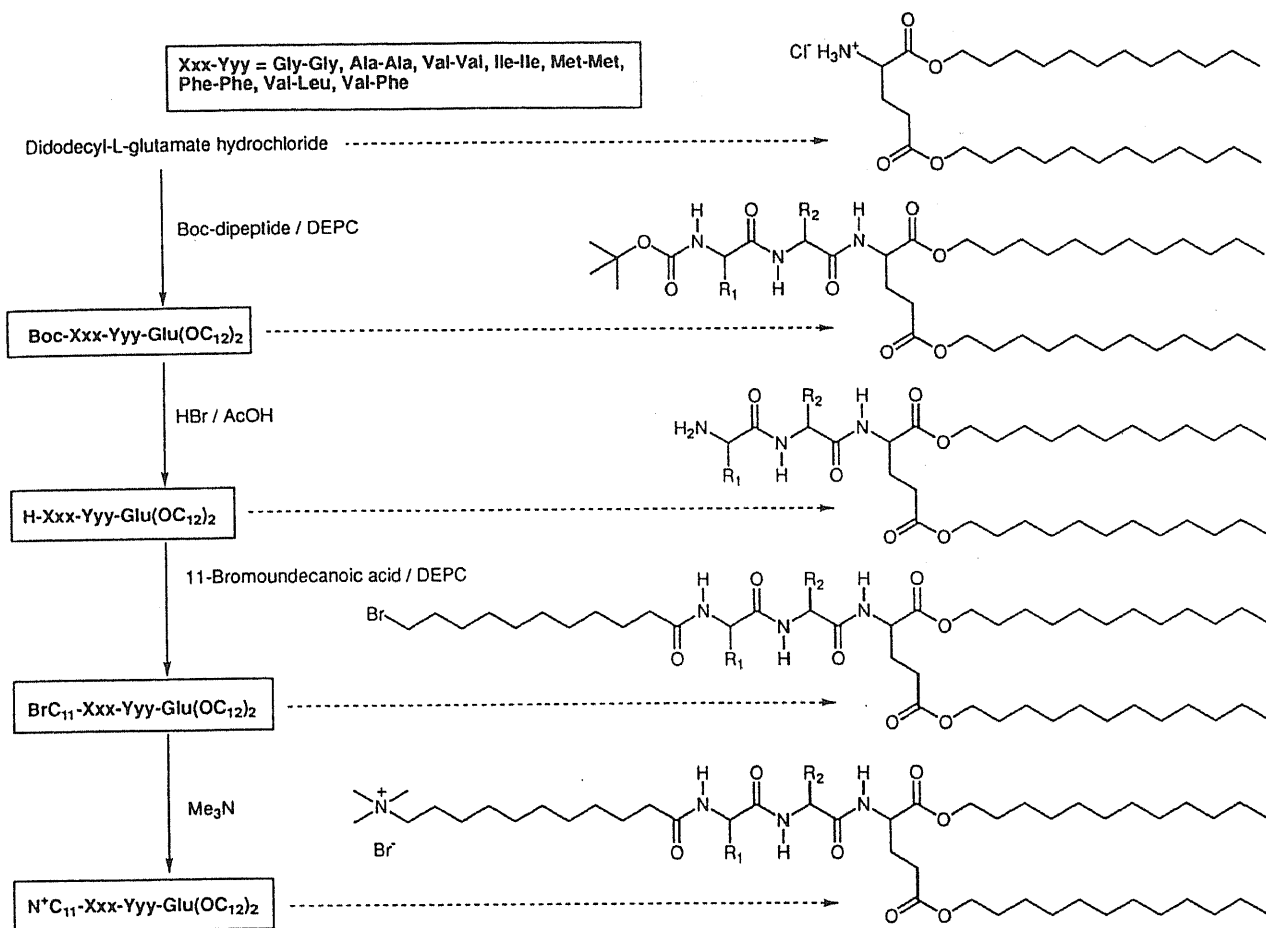


Chart 1

## 2.2 Preparation and Diagnostics

The tripeptide-containing amphiphiles can be easily prepared by the stepwise condensation of an *N*-protected amino acid with didodecyl-L-glutamate (Chart 1). The protective group, the *tert*-butyloxycarbonyl (Boc) group, was removed using HBr/acetic acid. The resulting tripeptide derivative was reacted with 11-bromoundecanoyl chloride followed by a quaternization reaction giving the tripeptide-containing amphiphiles. The details have been shown elsewhere.<sup>14</sup>

In the following section, we described not only the tripeptide-containing amphiphiles but also their intermediate molecules. We call the intermediates the hydrophobic tripeptide derivatives. Because the hydrophobic tripeptide derivatives include a tripeptide moiety, it seemed that they would be good amyloid models. However, this was wrong. The hydrophobic tripeptide derivatives did not self-assemble into an aggregate but assembled with an increase in concentration and/or a decrease in temperature.<sup>15</sup>

The tripeptide-containing amphiphiles used in this study can form only the  $\beta$ -sheet structure, because the  $\alpha$ -helix required at least 3.6 amino acid residues,<sup>16</sup> and the turn structure should be unfavorable for the normal bilayer

structure and the reversed bilayer structure. A problem is involved in the more rigorous analysis of the  $\beta$ -sheet structure. For example, CD spectroscopy should be the most general method to determine the secondary structure of peptides. However, CD spectroscopy cannot distinguish a parallel and an antiparallel  $\beta$ -sheet structure. On the other hand, an advantage of the Fourier transform infrared (FT-IR) method has been reported for the study of the dynamic properties of proteins in solution<sup>17,18</sup> and of synthetic oligopeptides in solution.<sup>19</sup> Using the FT-IR spectroscopy, we have established a method of diagnostics for these  $\beta$ -sheets.<sup>14, 20, 21</sup>

## 3 Static Properties of $\beta$ -Sheet Assemblage

First we describe the aggregate morphology and then discuss the amide modes in the assemblage. The morphology and the amide modes are the static properties of the assemblage. As described above, the tripeptide-containing amphiphiles formed an aggregate not only in water but also in organic solvents such as CCl<sub>4</sub>.<sup>12</sup> This ambidexterity was the most advantageous property of the molecules and was helpful in determining the  $\beta$ -sheet structure, be-

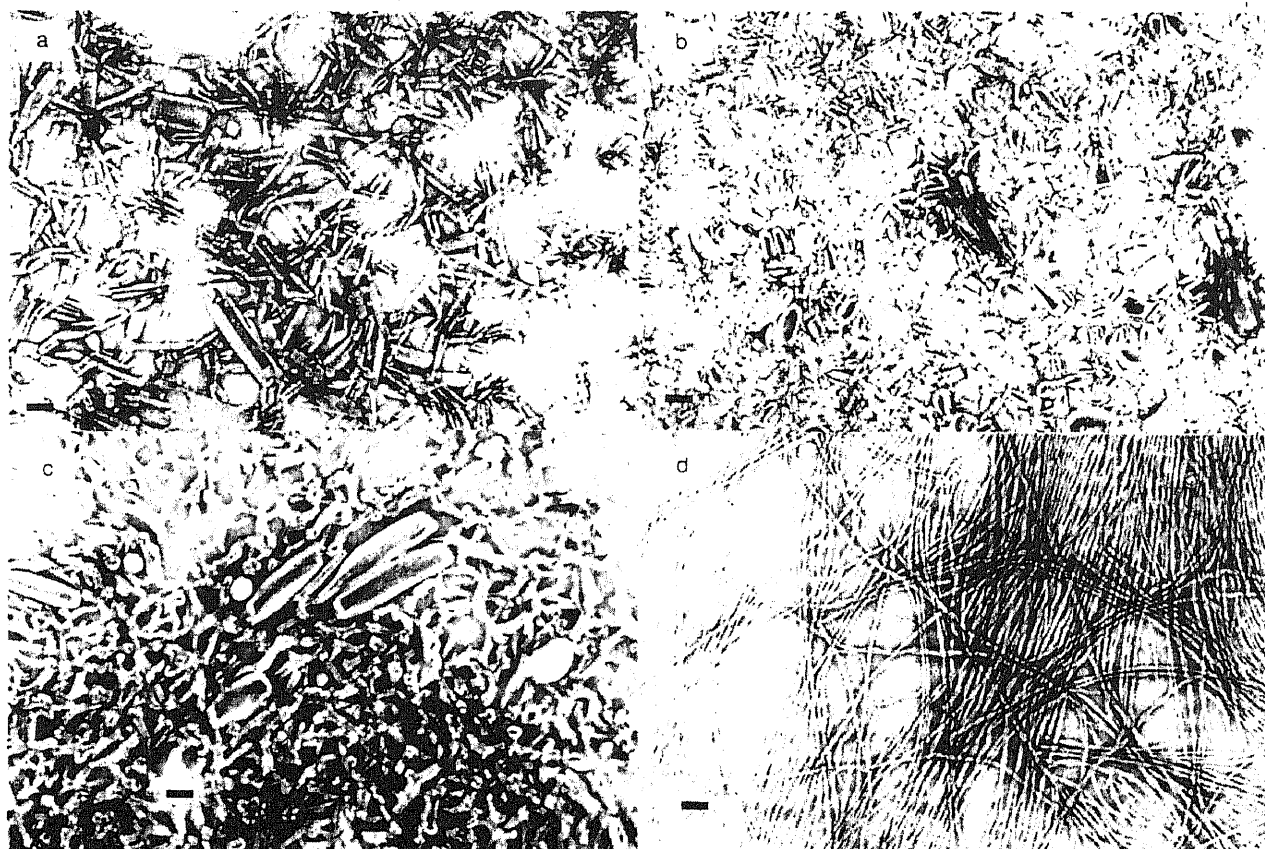


Figure 2 TEM images of the aqueous assemblages of (a)  $N^+C_{11}$ -Val-Val-Glu( $OC_{12}$ )<sub>2</sub>, (b)  $N^+C_{11}$ -Ile-Ile-Glu( $OC_{12}$ )<sub>2</sub>, (c)  $N^+C_{11}$ -Phe-Phe-Glu( $OC_{12}$ )<sub>2</sub>, and (d)  $N^+C_{11}$ -Ala-Ala-Glu( $OC_{12}$ )<sub>2</sub>, that were stained with 2%-uranylacetate (Scale bar; 1000 Å).

cause the aggregate structures within the aqueous and the organic media can be compared using the same molecule. Possessing two hydrophobic chains and a hydrophilic ammonium head, the amphiphile should form a bilayer structure in water (Figure 1(A')).<sup>9</sup> This molecular arrangement never forms an antiparallel  $\beta$ -sheet structure but forms a parallel  $\beta$ -sheet structure. The amide mode was entirely the same without respect to whether the solvent was water or  $CCl_4$  as described below. This result means that the local structure of the aggregate in organic solvents did not adopt an interdigitated structure (Figure 1(B')) but a reversed bilayer structure (Figure 1(C)). The normal and reversed bilayer structures contain the same molecular alignment in their half-layer and hence contained the same parallel  $\beta$ -sheet structure. There is controversy concerning the amide modes due to parallel  $\beta$ -sheet conformation because of the model polypeptide's lack of known x-ray structure for this conformation.<sup>22</sup> Therefore, the aggregate of the tripeptide-containing amphiphiles provides the model of the parallel  $\beta$ -sheet structure, which should contribute to the structural analyses of abnormal peptides.

### 3.1 Macroscopic Observations

All of the tripeptide-containing amphiphiles dissolved well in water giving a translucent solution. This is the typical exterior of an aqueous bilayer membrane. On the other hand, the amphiphiles formed a transparent gel when

they were dissolved in some nonpolar organic solvents. Table 1 summarizes the external appearance of the solutions of various organic solvents. A remarkable gel was observed when nonpolar organic solvents whose dielectric constant is in the range of 2.0–2.3 were employed.<sup>12</sup> It has been known that the organogel was a resultant product of the 3D networks of fibrous aggregates.<sup>25</sup> Therefore, the macroscopic observation as to whether or not the solution is a gel is a convenient method of determining the molecular aggregation. However, aggregate formation is not necessarily accompanied by gel formation, which means that the macroscopic observation will not give definitive evidence of the formation of molecular aggregates in organic solvents. Using Fourier transform infrared spectroscopy, we demonstrated more rigorous diagnostics of the aggregate formation as discussed in a later section (3.3).

### 3.2 Microscopic Observations

Aggregate morphology of the tripeptide-containing amphiphiles was revealed using a transmission electron microscope (TEM) and an atomic force microscope (AFM). Figure 2 includes the TEM images of the aggregates in water, where the aggregates were negatively stained with uranylacetate. A hollow tube, a distorted fiber or a helical fiber was observed with respect to the kind of the amino acid residue. Because the wall thickness of the tube and the diameter of the fiber is in the range 80 to 100 Å, which

**Table 1** External appearance of 2 mM-solutions of tripeptide-containing amphiphiles after 3 days incubation at room temperature

solvent	dielectric constant <sup>23</sup>	$N^+C_{11}\text{-Xxx-Yyy-Glu}(OC_{12})_2$						
		Gly-Gly	Ala-Ala	Val-Val	Ile-Ile	Phe-Phe	Val-Leu	Val-Phe <sup>24</sup>
n-hexane	1.8799 (25 °C)	insoluble	insoluble	insoluble	insoluble	insoluble	precipitation	precipitation
cyclohexane	2.023 (20 °C)	translucent solution	transparent gel	transparent gel	transparent gel	transparent gel	transparent gel	translucent gel
carbon tetrachloride	2.238 (25 °C)	translucent solution	transparent gel	transparent gel	transparent gel	transparent gel	transparent gel	translucent gel
benzene	2.275 (25 °C)	precipitation	transparent gel	transparent gel	transparent gel	transparent gel	transparent gel	transparent gel
toluene	2.379 (25 °C)	precipitation	transparent gel	transparent gel	transparent gel	transparent gel	transparent gel	transparent gel
chloroform	4.806 (20 °C)	transparent solution	transparent solution	transparent solution	transparent solution	transparent solution	transparent solution	transparent solution
ethyl acetate	6.02 (25 °C)	precipitation	precipitation	precipitation	precipitation	precipitation	transparent gel	precipitation
tetrahydrofuran	7.58 (25 °C)	precipitation	precipitation	transparent gel	transparent gel	transparent solution	transparent solution	precipitation
1, 1, 2, 2-tetrachloroethane	8.20 (20 °C)	transparent solution	transparent solution	transparent solution	transparent solution	transparent solution	transparent solution	transparent solution
acetone	20.70 (25 °C)	precipitation	precipitation	precipitation	precipitation	transparent solution	transparent solution	transparent solution
ethanol	24.55 (25 °C)	transparent solution	transparent solution	transparent solution	transparent solution	transparent solution	transparent solution	transparent solution
methanol	32.70 (25 °C)	transparent solution	transparent solution	transparent solution	transparent solution	transparent solution	transparent solution	transparent solution

**Figure 3** TEM images of the assemblage of  $N^+C_{11}\text{-Ala-Ala-Glu}(OC_{12})_2$  in different organic solvents (scale bar; 1000 Å): (a)  $CCl_4$ ; (b) benzene; (c) cyclohexane. Staining procedure was described elsewhere.<sup>14</sup>

corresponds to the extended bimolecular length of the tripeptide-containing amphiphiles ( $45 \text{ \AA} \times 2$ ), these aggregate should form a bilayer aggregate (Figure 1(A')).

Figures 3 and 4 show the TEM images of the aggregate in organic media. The aggregate morphology is generally a

fiber. The aggregate morphology was not dependent upon the kind of organic solvent but on the kind of the amino acid residue. For example, the amphiphile of  $N^+C_{11}\text{-Ala-Ala-Glu}(OC_{12})_2$  formed a straightforward fiber in  $CCl_4$ , benzene, and cyclohexane (Figure 3).<sup>14</sup> The small fibers observed in these images have a  $70\text{--}80 \text{ \AA}$  ( $7\text{--}8 \text{ nm}$ ) diam-

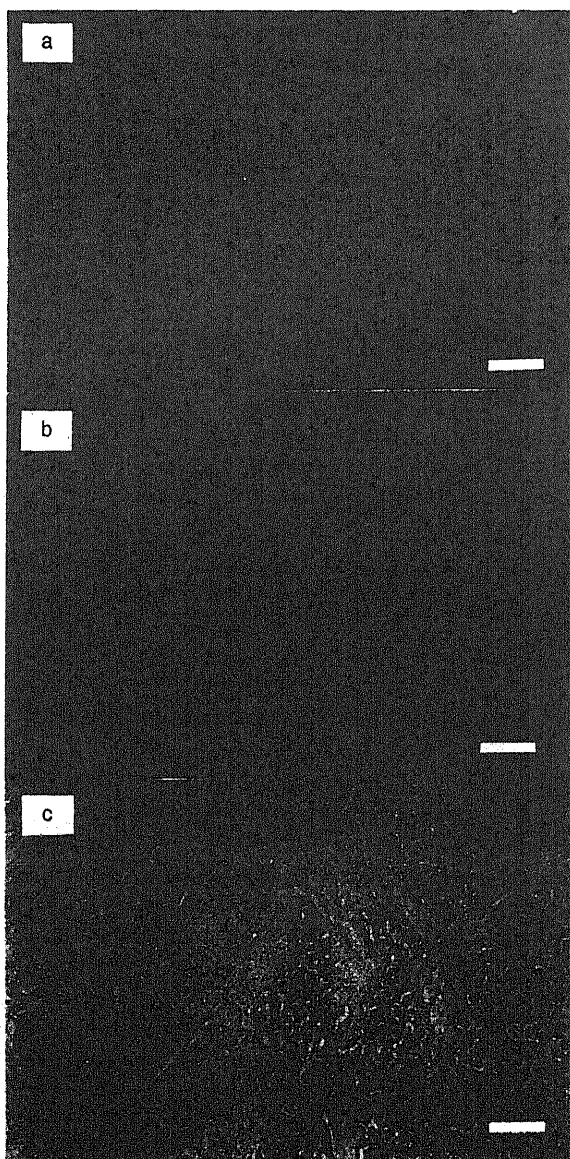


**Figure 4** TEM images of the assemblages of the tripeptide-containing amphiphiles in cyclohexane (2 mM): (a)  $N^+C_{11}\text{-Val-Val-Glu(OC}_{12})_2$ , (b)  $N^+C_{11}\text{-Ile-Ile-Glu(OC}_{12})_2$ ; (c)  $N^+C_{11}\text{-Phe-Phe-Glu(OC}_{12})_2$ . Scale bar is 2000 Å. Staining procedure was described elsewhere.<sup>14</sup>

eter. Because the expanded length of the molecule is 45 Å, the local structure of the aggregate in organic solvents did not adopt an interdigitated structure (Figure 1(B')) but a reversed bilayer structure (Figure 1(C)). The other amphiphiles formed a winding fiber, which sometimes formed spatially extended pseudo-crystalline microdomains which should be the node of the 3D network of the aggregate (Figure 4). We must not forget that these morphologies are very similar to the exterior of the amyloid fibril.

Three-dimensional figures of the aggregate were obtained using an AFM.<sup>14, 26, 27</sup> Recent development of atomic force microscopy (AFM) allows us to investigate the morphologies of molecular assemblies easily from a micrometer

scale to a molecular scale.<sup>28</sup> The AFM is now a powerful tool for investigating molecular assemblies. AFM measurement does not require sample pre-treatment such as staining; therefore, we can exclude artifact formation caused by the pre-treatment.<sup>29</sup> Another advantage in the AFM measurement is the easy evaluation of 3D morphologies. For example, we cannot judge only from TEM images whether the fibrous structures in Figures 3 and 4 have a round shape or a flat-tape-like structure. This problem is easily solved by applying AFM to the evaluation of the fibrous structure. Therefore, AFM observation would provide a large contribution of the evaluation of these fibrous structures. AFM images of the films cast on freshly cleaved mica were taken using a Nanoscope IIIa (Digital Instruments, Santa Barbara, CA) in the tapping mode in air. According to the manufacturer, the normal spring constant was 20–100 N m<sup>-1</sup>. The drive frequency was around 300 kHz. The scanning speed was at a line frequency of 1 Hz with 256 pixels per line. Figure 5 shows three-dimensional AFM images of the cast films of  $N^+C_{10}\text{-Ala-Ala-Glu(OC}_{12})_2$  from CCl<sub>4</sub>.<sup>14</sup> The AFM image confirms that the fibrous structure is not a flat tape. Thick trunk-like fibers and several branches are clearly seen. The narrowest branches have a width of 10–30 nm and a height of 10–20 nm. These values are relatively close to the diameter of fibers evaluated from the TEM image (7–8 nm). We have to consider that the size of small objects could be overestimated by the AFM, because the radius of the AFM tip is sometimes comparable to the size of the object. From the above-mentioned information, we can conclude that the AFM image represents the individual fibers and the fused bundles. This behavior might be regarded as a model of  $\beta$ -amyloid aggregation. It is important that similar exteriors were obtained using TEM and AFM, even if the samples were prepared by the different procedures. The TEM sample was fibers adsorbed onto an amorphous carbon film, whereas the AFM sample was a dried specimen of an organogel on mica. The effect of sample preparation on morphological observation sometimes causes artifact formation, when the aggregate and its components coexist at equilibrium.<sup>21</sup> Such aggregation behavior is characteristic for hydrophobic tripeptide derivatives described in a later section (4.1).

### 3.3 $\beta$ -Sheet Structure

Next, we studied the amide modes in the aggregate of the tripeptide-containing amphiphiles. Figure 6 is a typical example of the FT-IR spectra of  $N^+C_{11}\text{-Phe-Phe-Glu(OC}_{12})_2$  dissolved in different media.<sup>20</sup> The N-H stretching (amide A), the C=O stretching (amide I) and the N-H deformation (amide II) bands in a CHCl<sub>3</sub> solution (16 mM) absorbed at 3412, 1668 and 1497 cm<sup>-1</sup>, respectively (Figure 6(a)), indicating that hydrogen bonding was not formed. Such diagnostics were precisely described by Miyazawa et al.<sup>30</sup> This spectrum remained unchanged in the concentration range of 1–200 mM. In an aqueous and a CCl<sub>4</sub> solution, amide A and amide I appeared at lower frequencies with a sharpened peak contour, whereas

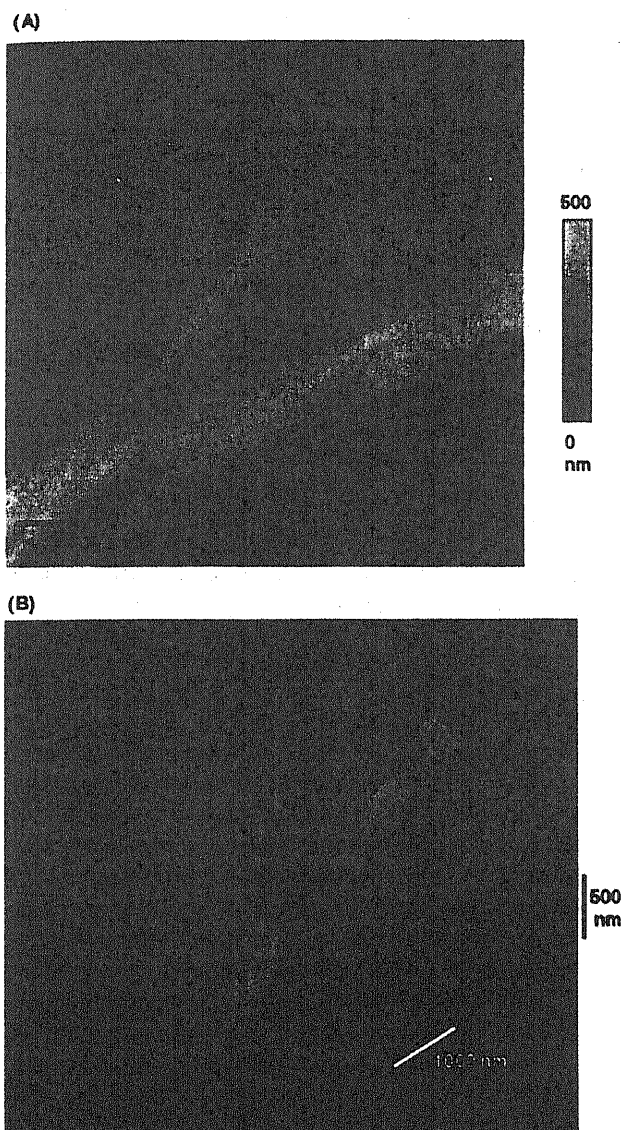


**Figure 5** AFM images of the air-dried cast film from  $\text{CCl}_4$  solution of  $\text{N}^+\text{C}_{11}\text{-Ala-Ala-Glu(OC}_{12})_2$ .<sup>14</sup>

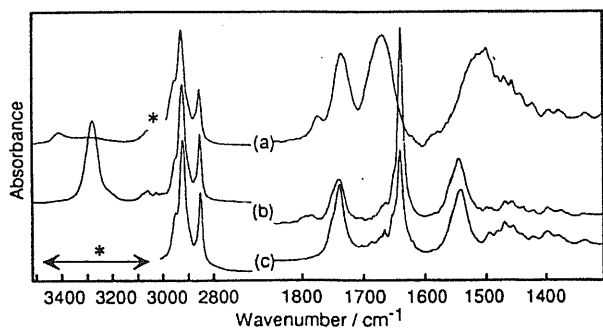


**Figure 6** FT-IR spectra of the tripeptide-containing amphiphile ( $\text{N}^+\text{C}_{11}\text{-Phe-Phe-Glu(OC}_{12})_2$ ) in different solvents: (a)  $\text{CHCl}_3$ ; (b)  $\text{CCl}_4$ ; (c) water. All spectra were measured at  $25.0 \pm 0.5$  °C.

\* It is impossible to subtract the solvent absorption in this region because of the strong  $\nu(\text{OH})$  band of water or of the  $\nu(\text{CH})$  band of  $\text{CHCl}_3$ . Experimental details were described elsewhere.<sup>20</sup>

**Table 2** Absorption frequencies of tripeptide-containing amphiphiles ( $\text{N}^+\text{C}_{11}\text{-Xxx-Yyy-Glu(OC}_{12})_2$ ) in different media<sup>14</sup>

tripeptide molecules	solvents <sup>a</sup>	spectral type <sup>b</sup>	frequencies / $\text{cm}^{-1}$		
			amide A	amide I	amide II
Val-Val	$\text{CCl}_4$	p- $\beta$	3280	1632	1546
Ile-Ile	$\text{CCl}_4$	p- $\beta$	3281	1632	1546
Phe-Phe	$\text{CHCl}_3$	N	3412	1668	1518
	$\text{CCl}_4$	p- $\beta$	3282	1637	1542
Met-Met	water	p- $\beta$	— <sup>c</sup>	1638	1538
	$\text{CCl}_4$	p- $\beta$	3280	1631	1543
Val-Leu	$\text{CHCl}_3$	N	3420	1664	1516
	$\text{CCl}_4$	p- $\beta$	3285	1634	1543
	water	p- $\beta$	— <sup>c</sup>	1635	1544

<sup>a</sup> Concentrations of the sample solutions were 1 mM for  $\text{CHCl}_3$  and  $\text{CCl}_4$  solution, and 20 mM for aqueous solutions. <sup>b</sup> N means a non-bonding amide mode, and p- $\beta$  means a parallel  $\beta$ -sheet structure (see Figure 7). <sup>c</sup> It is impossible to subtract the solvent absorption in this region because of the strong  $\nu(\text{O-H})$  band of water. Measurement temperature was  $25.0 \pm 0.5$  °C.

amide II appeared at a higher frequency (Figures 6 (b) and 6(c)). The remarkable band shifts show the presence of strong H-bonding within the aggregates both in water and in  $\text{CCl}_4$ . Similar treatment is possible to determine the aggregate formation if the molecule possesses at least one amide group. Emphasis is on the identity of the spectra of the aqueous and the  $\text{CCl}_4$  solutions in the region of 1500 and 1800  $\text{cm}^{-1}$ . In these solvents, the maximal wavenumbers of the amide I and II bands are located at 1637-1638 and 1538-1542  $\text{cm}^{-1}$ , respectively. Table 2 summarizes the maximal absorption frequencies of the amide A, amide I and amide II for the other tripeptide-containing amphiphiles.<sup>14</sup>

### 3.3.1 Parallel-Chain $\beta$ -Sheet Structure

The coincidence in the spectra given in Table 2 suggests that the modes of the H-bonding are the same irrespective of whether the solvent is water or  $\text{CCl}_4$ . Furthermore, the mode of the interpeptide H-bonding within the aggregates of the amphiphiles is independent of the amino acid structures except for  $\text{N}^+\text{C}_{11}\text{-Gly-Gly-Glu(OC}_{12})_2$  and  $\text{N}^+\text{C}_{11}\text{-Ala-Ala-Glu(OC}_{12})_2$ . Therefore, the FT-IR spectra of the aggregate of the tripeptide-containing amphiphiles were divided into three types as shown in Figure 7.<sup>14</sup>

The type I spectra which is the most general should be attributed to a parallel  $\beta$ -sheet structure for the following reasons: (1) the TEM images showed that the amphiphiles did not form an interdigitated structure without respect to the kinds of media. In the normal or reversed bilayer structure, an antiparallel  $\beta$ -sheet structure is never formed. The coincidence of the spectra in water and in  $\text{CCl}_4$  meant that the amphiphile should be arranged in the same manner; (2) the type I spectrum is very similar to those of *N*-deblocked-heptaphenylalanine, heptavaline and heptaiso-

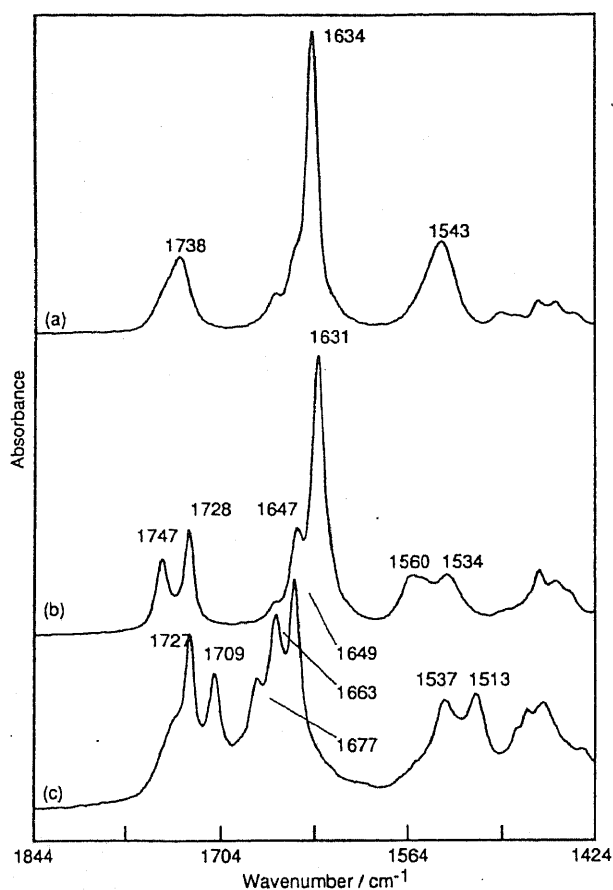


**Figure 7** FT-IR spectra of three different types of secondary structures of tripeptide-containing amphiphiles: (a) parallel  $\beta$ -sheet,  $\text{CCl}_4$  solution of  $\text{N}^+\text{C}_{11}\text{Val-Leu-Glu}(\text{OC}_{12})_2$  (1 mM); (b) pseudoparallel  $\beta$ -sheet,  $\text{CCl}_4$  solution of  $\text{N}^+\text{C}_{11}\text{Ala-Ala-Glu}(\text{OC}_{12})_2$  (1 mM); (c)  $\text{CCl}_4$  solution of  $\text{N}^+\text{C}_{11}\text{Gly-Gly-Glu}(\text{OC}_{12})_2$  (1 mM). Details were described elsewhere.<sup>14</sup>

leucine that can form a parallel  $\beta$ -sheet structure in the crystalline state.<sup>31</sup>

The type II spectrum was characteristic of  $\text{N}^+\text{C}_{11}\text{Ala-Ala-Glu}(\text{OC}_{12})_2$  in water and  $\text{CCl}_4$ , where the bands attributed to the ester, amide I and amide II split into two peaks. For example, the amide I band split into 1647 and 1631  $\text{cm}^{-1}$  (Figure 7). The presence of the major peak at 1631  $\text{cm}^{-1}$  and the absence of the weak band at about 1690  $\text{cm}^{-1}$  indicate the formation of a parallel  $\beta$ -sheet conformation. However, the band split, particularly at the ester carbonyl, suggests that one of the amide groups forms a hydrogen bond with either an  $\alpha$ - or a  $\gamma$ -ester group. We call this specific amide mode a pseudo-parallel  $\beta$ -sheet structure.<sup>13</sup>

The type III spectrum was observed in the  $\text{CCl}_4$  solutions of  $\text{N}^+\text{C}_{11}\text{Gly-Gly-Glu}(\text{OC}_{12})_2$ . The multiple peaks assigned to the amide I band meant that the amphiphile did not form any  $\beta$ -sheet structures. The amphiphile gave different spectra depending upon the conditions. In this aggregate, the H-bonding could be formed two-

dimensionally because glycinate residues possessed no sterically hindered side group.

### 3.3.2 Antiparallel-Chain $\beta$ -Sheet Structure

According to previous research, an antiparallel  $\beta$ -sheet structure provides a characteristic weak amide I band at about 1690  $\text{cm}^{-1}$  together with another strong amide I band at about 1630  $\text{cm}^{-1}$ . The former weak band has been inferred from the results of a theoretical calculation for the antiparallel  $\beta$ -sheet polypeptides<sup>22</sup> and observed in crystalline heptaalanine, heptanorvaline, heptaleucine, heptamethionine, and hepta-S-methylcysteine containing an antiparallel  $\beta$ -sheet structure.<sup>31</sup> In the cases of the heptapeptides, the major amide I band also appeared at a lower frequency (1630–1633  $\text{cm}^{-1}$ ) than that of the peptides forming a parallel  $\beta$ -sheet structure (1635–1639  $\text{cm}^{-1}$ ).<sup>31</sup> All of the tripeptide-containing amphiphiles gave no band at 1690  $\text{cm}^{-1}$ . However, an intermediate tripeptide derivative,  $\text{BrC}_{11}\text{-Ala-Ala-Glu}(\text{OC}_{12})_2$ , clearly showed the characteristic weak band at 1688  $\text{cm}^{-1}$  (Figure 8), when it was dissolved in  $\text{CCl}_4$ .<sup>14</sup> In this case, the hydrophobic  $\text{BrC}_{11}\text{-Ala-Ala-Glu}(\text{OC}_{12})_2$  formed an antiparallel  $\beta$ -sheet structure and should pack according to an interdigitated structure (Figure 1(B')) in  $\text{CCl}_4$ .

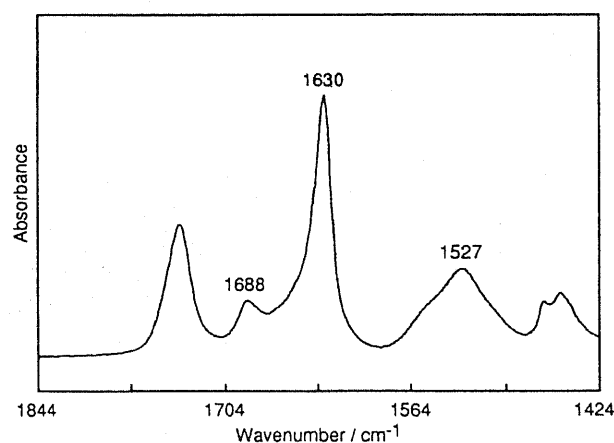


**Figure 8** FT-IR spectrum of antiparallel  $\beta$ -sheet structure: 10 mM- $\text{CCl}_4$  solution of  $\text{BrC}_{11}\text{Ala-Ala-Glu}(\text{OC}_{12})_2$ . Details were described elsewhere.<sup>14</sup>

## 4 Dynamic Properties of $\beta$ -Sheet Assemblage

As described above, we can diagnose the formation of the  $\beta$ -sheet assemblage by FT-IR spectroscopy. The FT-IR method is also suitable for real-time and continuous observation of molecular aggregation. The advantage of the FT-IR method is usefulness for detecting aggregate formation within a solution which is not a gel. Thus, we can study the critical concentration of aggregation, the thermal disintegration process of the aggregation, the transformation of the amide mode, and so on.

#### 4.1 Critical Concentration

Using FT-IR spectroscopy, we can estimate the critical concentration of aggregate formation.<sup>14,15,20</sup> We call the critical concentration C.A.C. that is likened to the conventional critical micellar concentration (C.M.C.). Figure 9 includes the FT-IR spectra of the  $\text{CCl}_4$  solution of  $\text{N}^+\text{C}_{11}\text{-Phe-Phe-Glu(OC}_{12})_2$  at four different concentrations.<sup>20</sup> Because subtraction of the  $\text{CCl}_4$  solvent becomes difficult at the lowest concentration, the degree of confidence of that spectrum could be lower than the others. However, the spectral pattern of the solution at 0.01 mM was the same as those of the solutions at higher concentrations that formed a typical parallel  $\beta$ -sheet structure. This result means that the amphiphile of  $\text{N}^+\text{C}_{11}\text{-Phe-Phe-Glu(OC}_{12})_2$  aggregated below  $10^{-5}$  mM. Because the  $\text{CCl}_4$  solution of  $\text{N}^+\text{C}_{11}\text{-Phe-Phe-Glu(OC}_{12})_2$  formed an apparent gel at a concentration of more than  $10^{-3}$  mM (ca. 1 mg/mL), molecular assembling has preceded formation of the gel. On the other hand, when tripeptide derivatives lack a hydrophilic head, for example,  $\text{Boc-Val-Val-Glu(OC}_{12})_2$ , stepwise aggregation was observed. Figure 10 shows the FT-IR spectra of the  $\text{CCl}_4$  solution of  $\text{Boc-Val-Val-Glu(OC}_{12})_2$  at different concentrations.<sup>15</sup> Although the tripeptide derivative did not form a parallel  $\beta$ -sheet structure in  $\text{CCl}_4$ , the C = O stretching modes of the ester, the urethane and the amide linkage were clearly assigned to 1738, 1692 and  $1649\text{ cm}^{-1}$ , respectively, for the thick solutions (10 and 20 mM). Boundaries between the bands of the urethane and the amide became unclear with a decrease in the concentration, giving a broad singlet band ( $1679\text{ cm}^{-1}$ ) for the thinnest solution (1 mM), which should be the absorption band attributed to the molecularly dispersed  $\text{Boc-Val-Val-Glu(OC}_{12})_2$ . The spectral change means that the aggregate formation was completed at 10 mM and that the monomeric species and the aggregate should coexist at equilibrium in the concentration range of 1–10 mM. A similar aggregation process was observed in the  $\text{CCl}_4$  solution of the other hydrophobic tripeptide derivatives, namely,  $\text{H-Val-Val-Glu(OC}_{12})_2$ ,  $\text{H-Phe-Phe-Glu(OC}_{12})_2$  and  $\text{Boc-Phe-Phe-Glu(OC}_{12})_2$ . These tripeptide derivatives aggregated at a concentration of about 10 mM, which is 1000 times that of the C.A.C. of the tripeptide-containing amphiphiles. Furthermore, these hydrophobic tripeptide derivatives hardly formed a gel if the concentration was increased to 100 mM or more.

#### 4.2 Thermal Stability

The presence of a hydrophilic ammonium group improved the thermal stability of the aggregates of the tripeptide derivatives. The thermal behavior of the aggregates in solution is usually studied by differential scanning calorimetry (DSC). We then performed DSC measurements on the  $\text{CCl}_4$  solutions of all the tripeptide derivatives. However, an exothermic and/or an endothermic peak was not observed for all of the tripeptide derivatives used in the study in the temperature range of 10–90 °C. This result meant that the solutions exhibited no phase transition in

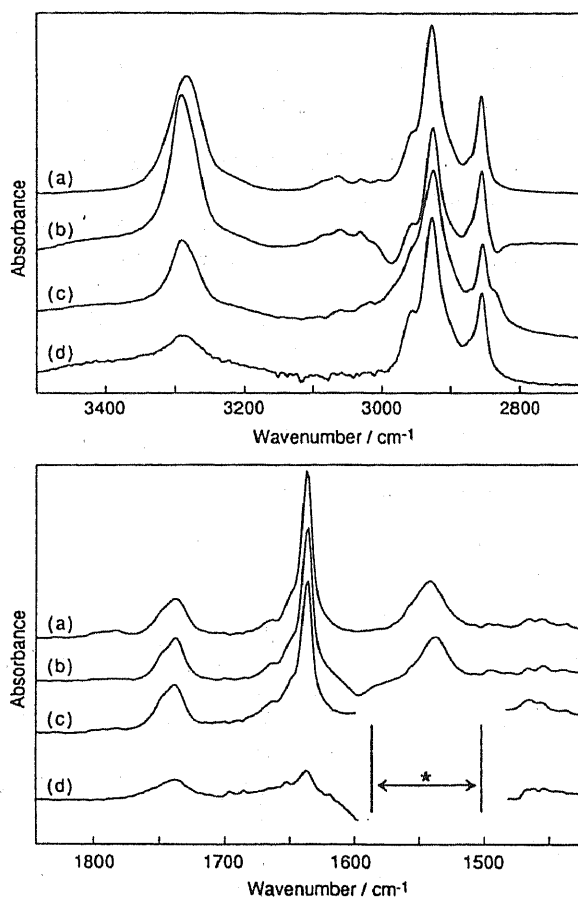


**Figure 9** FT-IR spectra of  $\text{CCl}_4$  solution of  $\text{N}^+\text{C}_{11}\text{-Phe-Phe-Glu(OC}_{12})_2$  in different concentrations: (a) 1 mM; (b) 0.5 mM; (c) 0.1 mM; (d) 0.01 mM. All spectra were measured at  $25.0 \pm 0.5$  °C. \* It is difficult to subtract the solvent absorption in these concentrations.

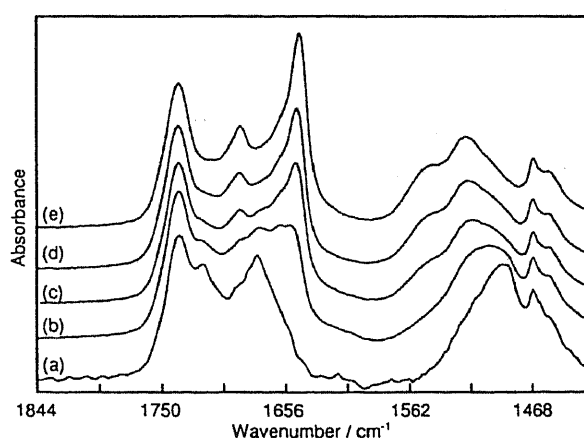


**Figure 10** Change in FT-IR spectra of  $\text{Boc-Val-Val-Glu(OC}_{12})_2$  versus the concentration in  $\text{CCl}_4$ : (a) 1 mM; (b) 5 mM; (c) 10 mM; (d) 20 mM; (e) 30 mM.

this temperature range. In fact, the FT-IR spectra of the  $\text{CCl}_4$  solution of  $\text{N}^+\text{C}_{11}\text{-Val-Val-Glu}(\text{OC}_{12})_2$  remained unchanged when the temperature was raised from 10 to 60 °C.<sup>14</sup> If a  $\text{CHCl}_3$  and  $\text{CCl}_4$  mixture was used as the solvent, we could observe the disintegration process of the aggregate of  $\text{N}^+\text{C}_{11}\text{-Phe-Phe-Glu}(\text{OC}_{12})_2$  due to increasing temperature (Figure 11).<sup>15</sup> The bottom spectrum in Figure 11 is attributed to the parallel-chain  $\beta$ -sheet structure of the tripeptide. The bonding amide I mode at  $1637\text{ cm}^{-1}$  quickly disappeared at temperatures above 55 °C and gave the same spectrum as that observed in  $\text{CHCl}_3$ .

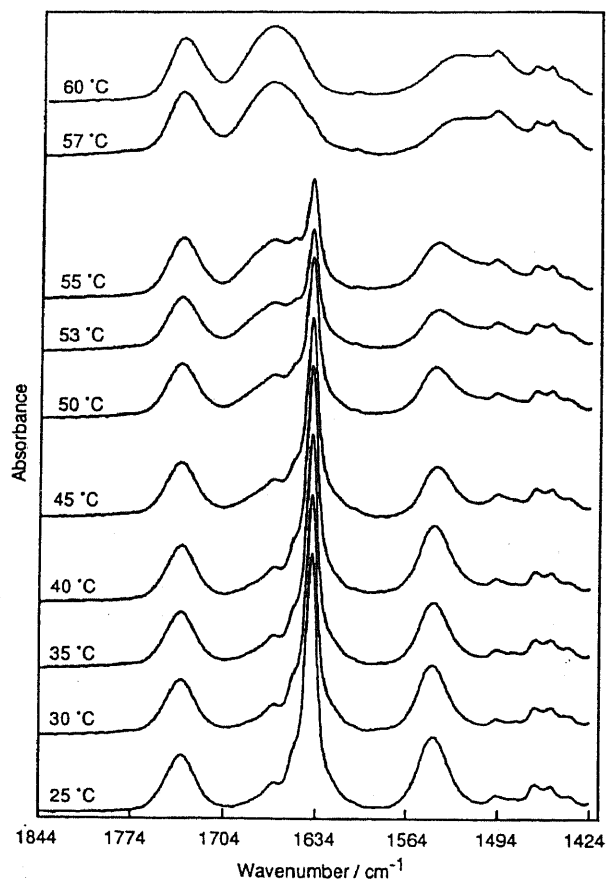


**Figure 11** Temperature dependence of FT-IR spectra of  $\text{N}^+\text{C}_{11}\text{-Phe-Phe-Glu}(\text{OC}_{12})_2$  in a 1:4 mixture of  $\text{CHCl}_3\text{-CCl}_4$  (4 mM).

On the other hand, the FT-IR spectra of the  $\text{CCl}_4$  solution of the hydrophobic tripeptides changed upon heating even if no endothermic peak was observed in the DSC thermogram. Figure 12 shows the temperature dependence of the FT-IR spectra of the  $\text{CCl}_4$  solution of  $\text{Boc-Val-Val-Glu}(\text{OC}_{12})_2$ .<sup>21</sup> Boundaries between the bands of the urethane and the amide became unclear with an increase in the temperature giving a broad singlet band ( $1679\text{ cm}^{-1}$ ) at the highest temperature (60 °C), which should be the absorption band attributed to the molecularly dispersed  $\text{Boc-Val-Val-Glu}(\text{OC}_{12})_2$ . The intensity of the bonding amide mode at  $1649\text{ cm}^{-1}$  gradually and continuously decreased with heating, which showed no critical temperature. Such

a disintegration process has never been detected by thermodynamic or rheologic observations, because the tripeptide derivative formed no gel in  $\text{CCl}_4$  over a wide temperature range.

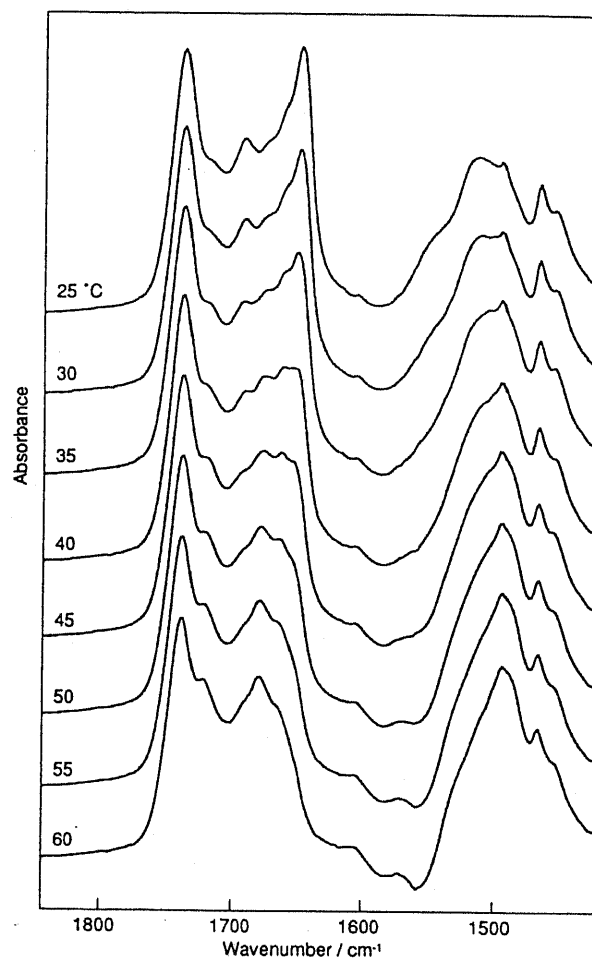


**Figure 12** Temperature dependence of FT-IR spectra of  $\text{CCl}_4$  solution of  $\text{Boc-Val-Val-Glu}(\text{OC}_{12})_2$ . Details were described elsewhere.<sup>20,21</sup>

We then compared the disintegration process of  $\text{Boc-Val-Val-Glu}(\text{OC}_{12})_2$  with that of  $\text{N}^+\text{C}_{11}\text{-Phe-Phe-Glu}(\text{OC}_{12})_2$ . As shown in Figure 13, the relative ratio of absorbance of the non-bonding ( $1678\text{ cm}^{-1}$ ) and the bonding amide I modes ( $1649\text{ cm}^{-1}$ ) continuously changed with increasing temperature within the aggregate of  $\text{Boc-Val-Val-Glu}(\text{OC}_{12})_2$ .<sup>15</sup> Therefore, the aggregation and disintegration of  $\text{Boc-Val-Val-Glu}(\text{OC}_{12})_2$  take place stepwise, which is strongly dependent upon concentration and temperature. On the other hand, the aggregate of  $\text{N}^+\text{C}_{11}\text{-Phe-Phe-Glu}(\text{OC}_{12})_2$  did not collapse up to the critical temperature. The ratio of absorbance of the non-bonding ( $1668.5\text{ cm}^{-1}$ ) and the bonding amide I modes ( $1637.5\text{ cm}^{-1}$ ) drastically increased at 55 °C, when the amphiphile  $\text{N}^+\text{C}_{11}\text{-Phe-Phe-Glu}(\text{OC}_{12})_2$  was dissolved in the  $\text{CHCl}_3\text{-CCl}_4$  mixture. Because the aggregate of  $\text{N}^+\text{C}_{11}\text{-Phe-Phe-Glu}(\text{OC}_{12})_2$  is stable over a wide temperature range and



formed at a very low concentration, only the aggregate should have spontaneous assemblage, while the other is the concentration-induced assemblage. The distinction between the two types of assemblages is very important when considering the driving force of the self-assembling in organic media.

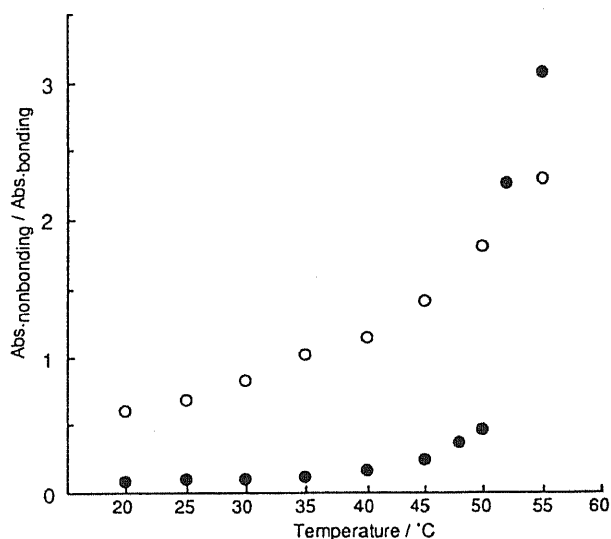


**Figure 13** Temperature dependence of the ratio of absorbance: solid circles are the ratio at 1668.5 (nonbonding) and 1637.5  $\text{cm}^{-1}$  (bonding) for a 4 mM-solution of  $\text{N}^+\text{C}_{11}\text{-Phe-Phe-Glu(OC}_{12})_2$  in a 1:4 mixture of  $\text{CHCl}_3\text{-CCl}_4$ ; open circles are the ratio at 1679 (nonbonding) and 1649  $\text{cm}^{-1}$  (bonding) for a 10 mM-solution of  $\text{Boc-Val-Val-Glu(OC}_{12})_2$  in  $\text{CCl}_4$ .

### 4.3 Catalyzing Effect

The parallel  $\beta$ -sheet could be transformed into an antiparallel counterpart when the molecule was mixed with other tripeptide-containing amphiphiles, for example,  $\text{C}_{13}\text{-Phe-Phe-PheOC}_{10}\text{N}^+$  and  $\text{C}_{13}\text{-Ala-Ala-AlaOC}_{10}\text{N}^+$  whose tripeptide part has an opposite direction (Chart 2). When the  $\text{N}^+\text{C}_{11}\text{-Ala-Ala-Glu(OC}_{12})_2$  was mixed with the single chain amphiphile ( $\text{C}_{13}\text{-Phe-Phe-PheOC}_{10}\text{N}^+$ ), a weak band at 1686  $\text{cm}^{-1}$ , which is evidence of an antiparallel  $\beta$ -sheet, appeared together with a strong amide I band at 1629  $\text{cm}^{-1}$  (Figure 14)<sup>14</sup> similar to that of the tripeptide molecule  $\text{BrC}_{11}\text{-Ala-Ala-Glu(OC}_{12})_2$  (Figure 8). The  $\text{C}_{13}\text{-Phe-Phe-PheOC}_{10}\text{N}^+$  alone, of course, formed a parallel  $\beta$ -sheet. On the other hand, it was possible to reform the pseudo-parallel  $\beta$ -sheet structure of  $\text{N}^+\text{C}_{11}\text{-Ala-Ala-Glu(OC}_{12})_2$  into a parallel  $\beta$ -sheet structure. In this case, the pseudo-parallel  $\beta$ -sheet structure of  $\text{N}^+\text{C}_{11}\text{-Ala-Ala-Glu(OC}_{12})_2$  transformed into a parallel  $\beta$ -sheet structure on mixing with a parallel  $\beta$ -sheet-forming  $\text{N}^+\text{C}_{11}\text{-Phe-Phe-Glu(OC}_{12})_2$ . The transformations between secondary structures are associated with the natural amyloid formation, because it is believed that a segment of a protein in the  $\beta$ -sheet form, especially a prion peptide, catalyzes the further conversion of segments from an  $\alpha$ -helix to the  $\beta$ -sheet form.<sup>1,8</sup>

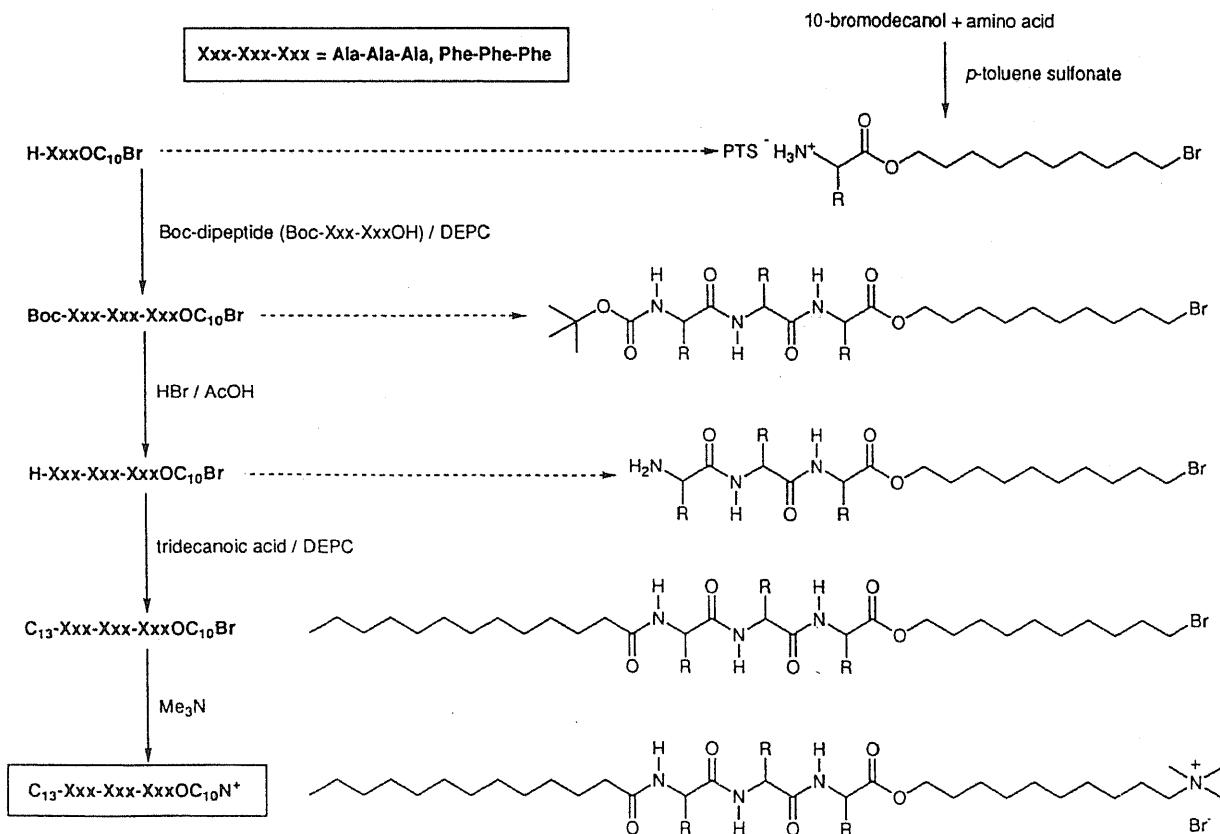
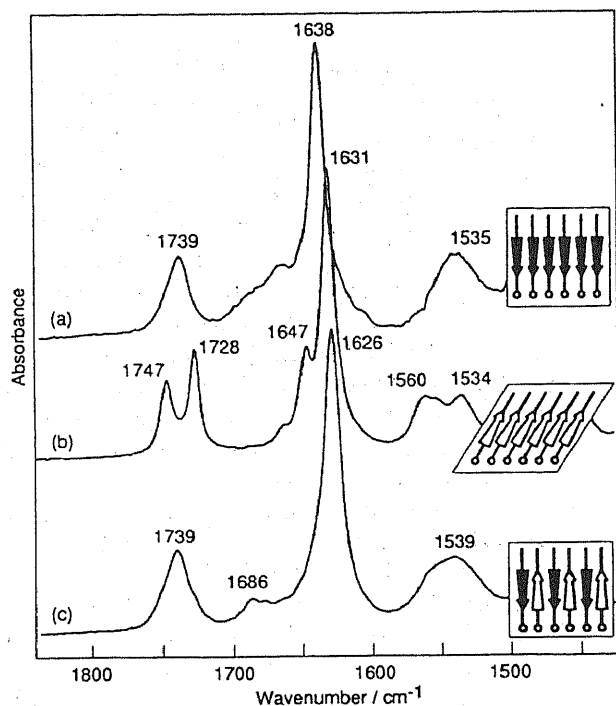


Chart 2



**Figure 14** FT-IR spectra of binary mixture and respective components in  $\text{CCl}_4$  solution: (a)  $\text{C}_{13}$ -Phe-Phe-PheOC $_{10}\text{N}^+$ ; (b)  $\text{N}^+\text{C}_{11}$ -Ala-Ala-Glu(OC $_{12}$ ) $_2$ ; (c) binary mixture.

#### 4.4 Hydrophobic Tripeptide Derivatives

As described in the previous sections, the amphiphilic and hydrophobic tripeptide derivatives were different with regard to their aggregation processes. The aggregate of the hydrophobic tripeptide derivatives was formed stepwise with an increase in concentration and continuously disintegrated on heating. Hence, the morphology of this aggregate easily changes by condensation of the solution, which is the reason why we do not show the aggregate morphology of the aggregates. The details have been reported elsewhere.<sup>21</sup>

## 5 Conclusion

We have demonstrated that the aggregate of the tripeptide-containing amphiphiles possessed static and dynamic properties very similar to those of the amyloid fibril. Although the pathogeny of amyloidosis has progressed for some time, the therapy has been forestalled. The most serious problem of amyloidosis involves neurodegeneracy, especially dementia. If the symptoms are delayed even for one year, many people should be relieved of mental and physical pain. We believe that elimination or destruction of the  $\beta$ -sheet assemblage should be an effective medical treatment for the disease. Using this model, we are now seeking a molecule that destroys the  $\beta$ -sheet assemblage.

## References and Notes

- (1) Prusiner, S. B. *Science* **1997**, *278*, 245-251.
- (2) Borman, S. *Chem. Eng. News* **1999**, *7*.
- (3) Inouye, H.; Fraser, P. E.; Kirschner, D. A. *Biophys. J.* **1993**, *64*, 502-519.
- (4) Symmons, M. F.; Buchanan, S. G. St. C.; Clarke, D. T.; Jones, G.; Gay, N. J. *FEBS Lett.* **1997**, *412*, 397-403.
- (5) Zhang, S.; Rich, A. *Proc. Natl. Acad. Sci.* **1997**, *94*, 23-28.
- (6) Aggeli, A.; Bell, M.; Boden, N.; Keen, J. N.; Knowles, P. F.; McLeish, T. C. B.; Pitkeathly, M.; Radford, S. E. *Nature* **1997**, *386*, 259-262.
- (7) Kirschner, D. A.; Inouye, H.; Duffy, L. K.; Sinclair, A.; Lind, M.; Selkoe, D. J. *Proc. Natl. Acad. Sci. USA* **1987**, *84*, 6953-6957.
- (8) Gasset, M.; Baldwin, M. A.; Lloyd, D. H.; Gabriel, J.-M.; Holtzman, D. M.; Cohen, F.; Fletterick, R.; Prusiner, S. B. *Proc. Natl. Acad. Sci. USA* **1992**, *89*, 10940-10944.
- (9) Kunitake, T. *Angew. Chem. Int. Ed. Engl.* **1992**, *31*, 709-726.
- (10) K. Okuyama, M. Shimomura, *New Developments in Construction and Function of Organic Thin Films*, (Eds.: T. Kajiyama and M. Aizawa), Elsevier Science B. V., 39-70 **1996**.
- (11) Yamada, N.; Okuyama, K.; Serizawa, T.; Kawasaki, M.; Oshima, S. *J. Chem. Soc., Perkin 2* **1996**, 2707-2713.
- (12) Yamada, N.; Koyama, E.; Kaneko, M.; Seki, H.; Ohtsu, H.; Furuse, T. *Chem. Lett.* **1995**, 387-388.
- (13) Yamada, N.; Koyama, E.; Maruyama, K. *Kobunshi Ronbunshu* **1995**, *52*, 629-638.
- (14) Yamada, N.; Ariga, K.; Naito, M.; Matsubara, K.; Koyama, E. *J. Am. Chem. Soc.* **1998**, *120*, 12192-12199.
- (15) Yamada, N.; Matsubara, K.; Koyama, E.; Fujioka, M. *Chem. Lett.* **1997**, 1033-1034.
- (16) Stryer, L. In *Biochemistry*, 3rd ed.; W. H. Freeman and Company: New York, 1988.
- (17) Susi, H.; Byler, D. M. *Arch. Biochem. Biophys.* **1987**, *258*, 465-469.
- (18) Surewicz, W. K.; Mantsch, H. H. *Biochim. Biophys. Acta* **1988**, *952*, 115-130.
- (19) Dieudonné, D.; Gericke, A.; Flach, C. R.; Jiang, X.; Farid, R. S.; Mendelsohn, R. *J. Am. Chem. Soc.* **1998**, *120*, 792-799.
- (20) Yamada, N.; Koyama, E.; Imai, T.; Matsubara, K.; Ishida, S. *J. Chem. Soc., Chem. Commun.* **1996**, 2297-2298.
- (21) Yamada, N.; Matsubara, K.; Narumi, K.; Sato, Y.; Koyama, E.; Ariga, K., *Colloids Surf.*, A in press.
- (22) Bandekar, J. *Biochim. Biophys. Acta* **1992**, *1120*, 123-143.
- (23) Riddick, J. A.; Bunger, W. B. In *Organic Solvents*, 3rd ed.; Wiley-Interscience, New York, 1970.
- (24) Yamada, N.; Nishigai, Y. unpublished result.
- (25) Terech, P.; Weiss, R. G. *Chem. Rev.* **1997**, *97*, 3133-3159.
- (26) Ariga, K.; Yamada, N.; Naito, M.; Koyama, E.; Okahata, Y. *Chem. Lett.* **1998**, 493-494.
- (27) Ariga, K.; Kikuchi, J.; Narumi, K.; Koyama, E.; Yamada, N. *Chem. Lett.* **1999**, 787-788.
- (28) Shao, Z.; Mou, J.; Czajkowsky, D. M.; Yuan, J. -Y. *Adv. Phys.* **1996**, *45*, 1-86.
- (29) Lukac, S.; Perovic, A. *J. Colloid Interface Sci.* **1985**, *103*, 586-589.
- (30) Masuda, Y.; Fukushima, K.; Fujii-Imae, T.; Miyazawa, T. *Biopolymers* **1969**, *8*, 91-99.
- (31) Toniolo, C.; Palumbo, M. *Biopolymers* **1977**, *16*, 219-224.

Article Identifier:

1437-2096,E;2000,0,05,0575,0586,ftx,en;A24099ST.pdf